

THESIS FOR THE DEGREE OF DOCTOR OF PHILOSOPHY

**Weldability of Precipitation Hardening Superalloys –
Influence of Microstructure**

JOEL ANDERSSON

Materials Technology Department
Volvo Aero Corporation

Department of Materials and Manufacturing Technology
CHALMERS UNIVERSITY OF TECHNOLOGY
Göteborg, Sweden, 2011

Weldability of Precipitation Hardening Superalloys – Influence of Microstructure

JOEL ANDERSSON
ISBN 978-91-7385-546-4

© JOEL ANDERSSON, 2011.

Doktorsavhandlingar vid Chalmers Tekniska Högskola
Ny serie nr 3227
ISSN 0346-718X

Department of Materials and Manufacturing Technology
Chalmers University of Technology
SE-412 96 Göteborg, Sweden
Tel: + 46 (0)31-772 1000
www.chalmers.se

Printed and bound by Chalmers Reproservice
Göteborg, Sweden, 2011

As always

To my wife Alma - Yes I Love Her

Weldability of Precipitation Hardening Superalloys – Influence of Microstructure

JOEL ANDERSSON

Department of Materials and Manufacturing Technology
Chalmers University of Technology

ABSTRACT

Superalloys and in particular the precipitation hardened Ni-based superalloys have always been used extensively in the hot sections of jet engines. Large hot structural engine components with complex geometry have preferably been cast as single piece components since the large scale vacuum investment casting process became available about fifty years ago. However, a recent trend is to cast smaller pieces which can be joined with sheet or forged parts to fabricate structural components. The rationale for this fabrication strategy is the possibility to save weight by the use of higher strength wrought material, where geometry allows, and join these wrought parts with cast material where complex geometry is needed and where the demand for strength is moderate. One of the major challenges using this strategy is the obvious fact that numerous welds must be made which requires the fundamental understanding, not least metallurgical, of how different materials may be joined by specific welding processes.

The main objective of this research has, for this reason, been to examine and interpret the weldability of precipitation hardened superalloys from a metallurgical standpoint. Two newly developed superalloys Allvac[®] 718Plus[™] and Haynes[®] 282[®] are compared with the two well established Alloy 718 and Waspaloy. The understanding of the influence of secondary phases such as carbides and δ phase in the microstructure was addressed by systematic hot ductility testing (Gleeble) and by weldability testing (Varestraint). The effect of secondary phases were also analysed through practical welding as by electron beam welding (EBW), and by gas tungsten arc welding (GTAW). The research showed that all the techniques used (Varestraint testing, Gleeble testing, DSC thermal analysis and welding (GTAW repair and EBW)) in studying the weldability independently provided important knowledge and most importantly that a combination of the results from these different techniques were necessary for the understanding of the weldability of these four alloys. From a microstructural point of view it has been possible to show that δ phase contrary to what has generally been assumed improves the weldability due to its ability to inhibit grain growth and to assist in the healing of cracks.

For future research, a new modified weldability testing method was developed where it is possible to perform Varestraint, Transvarestraint and spot-varestraint testing at ram speeds from 15 to 300 mm/s using GTAW, plasma arc welding and laser welding.

Keywords: Gleeble testing, Varestraint testing, Transvarestraint testing, DSC thermal analysis, Hot cracking, Solidification cracking, HAZ liquation cracking, Strain age cracking, Repair welding, GTAW, EBW

PREFACE

This doctoral thesis is a summary of work that has been performed at the Department of Materials and Manufacturing Technology (Chalmers University of Technology) and the Department of Materials Technology (Volvo Aero Corporation), July 2006 - June 2011.

Project funding was provided by KME (**KME-406** and **KME-506**) which is a consortium for materials technology directed towards thermal energy processes, CAPE graduate school in advanced production engineering and VITAL. VITAL was a European collaborative research project, running for four years, which aims to significantly reduce aircraft engine noise and CO₂ emissions.

The thesis consists of an introductory text which summarizes existing theories and the research which was carried out and reported in detail in the nine appended papers as shown below.

APPENDED PAPERS:

- Paper I Solidification Cracking of Alloy Allvac[®] 718Plus[™] and Alloy 718 at Transvarestraint Testing**
J. Andersson, G. Sjöberg, A. Brederholm, and H. Hänninen
The Minerals, Metals and Materials Society (TMS) 137th Annual Meeting, Proceedings of Sessions and Symposia Sponsored by the Extraction and Processing Division (EPD) Congress, ed. by S. M. Howard, New Orleans, USA, March, 2008, pp. 157 – 169.
- Paper II Hot Cracking of Allvac[®] 718Plus[™], Alloy 718 and Waspaloy at Varestraint testing**
J. Andersson, G. Sjöberg, L. Viskari, A. Brederholm, H. Hänninen, and C. S. Knee
Proceedings of the 47th Conference of Metallurgists (COM), ed. by. M. Elboujdaini, Winnipeg, Canada, August, 2008, pp. 401 – 413.
- Paper III Hot Ductility Study of Haynes[®] 282[®] Superalloy**
J. Andersson, G. Sjöberg, and M. C. Chaturvedi
Proceeding of The 7th International Symposium on Superalloy 718 and Derivatives, TMS (The Minerals, Metals and Materials Society), ed. by E. A. Ott, J. R. Groh, A. Banik, I. Dempster, T. P. Gabb, R. Helmink, X. Liu, A. Mitchell, G. P. Sjöberg, and A. Wusatowska-Sarnek, October, 2010, pp. 539-554.

- Paper IV Investigation of Homogenization and its Influence on the Repair Welding of Cast Allvac® 718Plus™ Superalloy**
J. Andersson, G. Sjöberg, and J. Larsson
Proceedings of The 7th International Symposium on Superalloy 718 and Derivatives, TMS (The Minerals, Metals and Materials Society), ed. by E. A. Ott, J. R. Groh, A. Banik, I. Dempster, T. P. Gabb, R. Helmink, X. Liu, A. Mitchell, G. P. Sjöberg, and A. Wusatowska-Sarnek, October, 2010, pp.439-454.
- Paper V Metallurgical Response of Electron Beam Welded Allvac® 718Plus™**
J. Andersson, G. Sjöberg, and H. Hänninen
Hot Cracking Phenomena in Welds III, Ed. by T.H. Boellinghaus, J.C. Lippold, and C.E. Cross, ISBN 978-3-642-16863-5, 2011.
- Paper VI Effect of Different Solution Heat Treatments on the Hot Ductility of Superalloys, Part 1 - Alloy 718**
J. Andersson, G. Sjöberg, L. Viskari, and M. C. Chaturvedi
(Submitted to Materials Science and Technology)
- Paper VII Effect of Different Solution Heat Treatments on the Hot Ductility of Superalloys, Part 2 - Allvac® 718Plus™**
J. Andersson, G. Sjöberg, L. Viskari, and M. C. Chaturvedi
(Submitted to Materials Science and Technology)
- Paper VIII Effect of Different Solution Heat Treatments on the Hot Ductility of Superalloys, Part 3 - Waspaloy**
J. Andersson, G. Sjöberg, L. Viskari, and M. C. Chaturvedi
(Submitted to Materials Science and Technology)
- Paper IX Repair Welding of Wrought Superalloys – Alloy 718, Allvac® 718Plus™ and Waspaloy**
J. Andersson, and G. Sjöberg
(Submitted to Science and Technology of Welding and Joining)

CONTRIBUTIONS TO THE APPENDED PAPERS

I've written all papers in close cooperation with my supervisor, Prof. Göran Sjöberg. The process has started with me writing the draft followed by suggestions from my supervisor and co-authors whereas I've finalized the specific papers.

Paper I I performed the Transvarestraint testing and scanning electron microscopy SEM analysis together with Anssi Brederholm and Kenneth Andersson (Volvo Aero), respectively. I carried out the metallographic preparations and the light optical microscopy (LOM) analysis.

Paper II I performed the Varestraint testing, (SEM) and differential scanning calorimetry (DSC) analysis together with Anssi Brederholm, Leif Viskari and Christopher Knee (Göteborg University), respectively. I carried out the metallographic preparations and the LOM.

Paper III I carried out all experimental work.

Paper IV I performed the heat treatments, weld test-plate preparation and crack measurements. The macro-etching was performed together with Per Göthe and Pia Olsson at Volvo Aero whereas metallography in terms of LOM and SEM together with Josefin Larsson (co-author) and Björn Karlsson (Volvo Aero), respectively.

Paper V I did the SEM analyses together with Tapio Saukkonen (Aalto University) and performed most of the metallographic preparations and the LOM analyses by myself.

Paper VI-VIII performed all the metallographic preparations and LOM analyses, heat treatments, hardness and Gleeble tests. I did the SEM and DSC work together with Leif Viskari and Christopher Knee, respectively.

Paper IX I did all experimental work except the SEM which was carried out together with Björn Karlsson (Volvo Aero) and the actual repair welding operations which were performed by experienced welders at Volvo Aero.

Beside the appended papers, the following papers have been published within the scope of the research project but are not included in the thesis:

Notch Sensitivity and Intergranular Crack Growth in the Allvac[®] 718Plus[™] Superalloy

J. Andersson, G. Sjöberg, and S. Hatami

Proceedings of International Society for Airbreathing Engines (ISABE), Beijing, China, September, 2007, n.1293.

New Materials in the Design and Manufacturing of Hot Structures for Aircraft Engines - Allvac® 718Plus™

G. Sjöberg, J. Andersson, and A. Sjunnesson

Proceedings of International Society for Airbreathing Engines (ISABE), Montreal, Canada, September, 2009, n.1286.

TABLE OF CONTENTS

1 Introduction	1 -
1.1 Background	2 -
1.2 Aim.....	3 -
1.2.1 Objectives.....	4 -
2 Aerospace Superalloys	5 -
2.1 Manufacturing of Superalloys	5 -
2.2 Physical Metallurgy of Superalloys.....	5 -
2.2.1 The γ Matrix Phase	7 -
2.2.2 The Precipitation Strengthening Phases - γ' and γ''	7 -
2.2.3 Carbides.....	7 -
2.2.4 Other Phases	8 -
2.3 Heat Treatments	8 -
3 Welding and Weldability of Aerospace Superalloys	11 -
3.1 Gas Tungsten Arc Welding	11 -
3.2 Electron Beam Welding	11 -
3.3 Residual Stresses in Welding.....	12 -
3.4 Weld Cracking.....	12 -
3.4.1 Solidification Cracking	13 -
3.4.2 Heat Affected Zone Liquation Cracking.....	16 -
3.4.3 Strain Age Cracking.....	19 -
3.5 Weldability Testing	20 -
3.5.1 Representative Tests.....	21 -
3.5.2 Gleeble Hot Ductility Test	21 -
3.5.3 The Varestraint Test and Derivatives.....	25 -
4 Experimental Procedures	29 -
4.1 Materials and Heat Treatments	29 -
4.1.1 Alloy 718	29 -
4.1.2 ATI Allvac [®] 718Plus [™]	30 -
4.1.2 Waspaloy.....	32 -

4.1.2 Haynes® 282®	- 33 -
4.2 Metallographic Procedures	- 33 -
4.3 Microscopy.....	- 33 -
4.4 Differential Scanning Calorimetry	- 34 -
4.5 Hardness Testing	- 34 -
4.6 Welding	- 34 -
4.6.1 EB Welding.....	- 34 -
4.6.2 Repair Welding	- 35 -
4.7 Vareststraint and Transvareststraint Testing	- 35 -
4.8 Gleeble Testing.....	- 36 -
5 Summary of Results in Appended Papers.....	- 37 -
5.1 Paper I and II.....	- 37 -
5.2 Paper III.....	- 39 -
5.3 Paper IV	- 41 -
5.4 Paper V	- 44 -
5.5 Paper VI-VIII.....	- 46 -
5.6 Paper IX	- 50 -
6 Concluding Remarks	- 51 -
6.1 Conclusions.....	- 51 -
6.2 Industrial and Scientific Contribution	- 52 -
7 Future Work.....	- 53 -
Acknowledgements.....	- 55 -
References.....	- 57 -

Chapter 1

1 Introduction

Superalloys and in particular the precipitation hardening Ni-based superalloys have been used extensively in the hot sections of jet engines since the introduction in the mid 20th century. In figure 1, a modern jet engine is shown together with high-lighted parts belonging to the specialization of Volvo Aero Corporation (VAC). The parts located at the rear end of the engine are made of superalloys both in modern aircraft engines and in land based gas turbines due to their remarkable high temperature strength capabilities. Here Alloy 718 is the standard and versatile alloy which can be used up to 650 °C without losing significant strength.

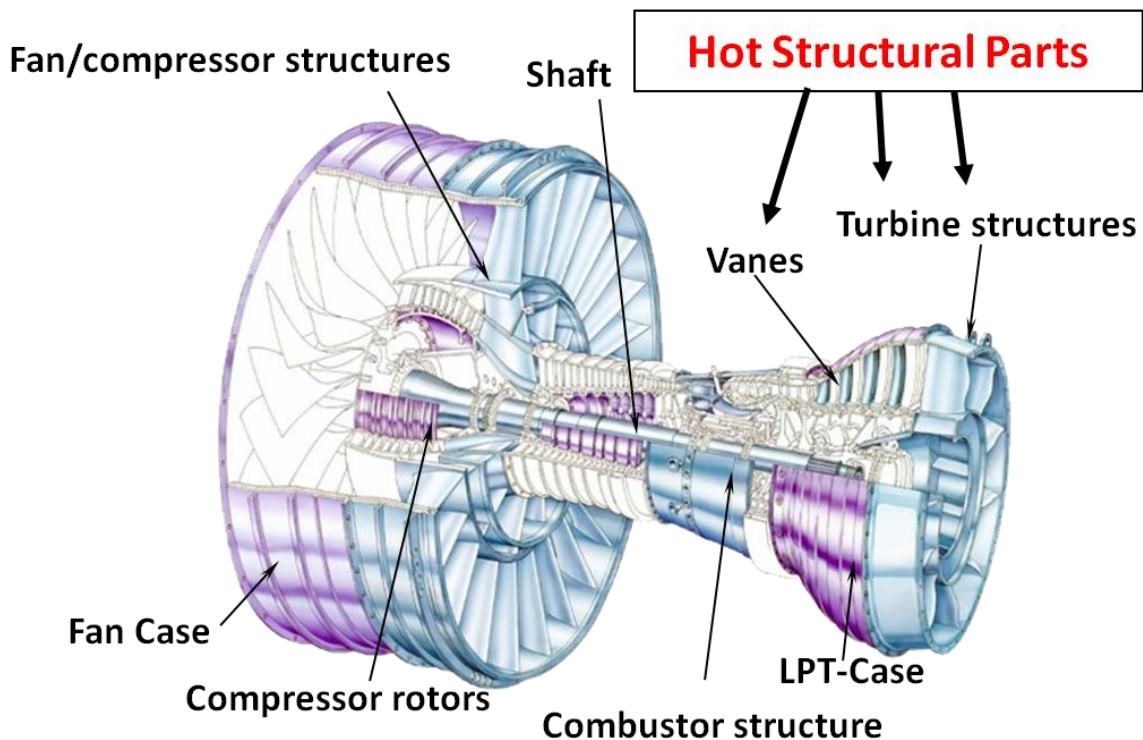


Figure 1. High by-pass commercial aircraft engine together with high-lighted components which belong to the product specialization of Volvo Aero Corporation.

The high temperature properties of these alloys are outstanding and are not challenged by any other alloy system. This is also the main reason why they are used since the cost is not in their favor, at least not when compared to steel. To reduce the overall costs of operating the engines and to reduce the environmental impact the service temperature of the engines are constantly increased. Today, the turbine inlet gas temperature in a modern engine can be as high as 1500 °C which is accomplished by

the use of sophisticated single crystal superalloys blades with incorporated cooling systems¹. However, these turbine blade materials are alloyed and manufactured in a way that makes these materials impossible to be used in large structural components as the ones seen in figure 1. The task is then to develop superalloys suitable for structural applications with higher service temperatures but at the same time as easy to manufacture as Alloy 718.

It goes without saying that alloy development must go hand in hand with the understanding of different manufacturing processes and in particular the welding process which is very important in the manufacturing of the large hot structural parts as the ones seen in figure 1.

1.1 Background

Volvo Aero is part of the Volvo Group company and produces large and advanced hot structural components for the aerospace industry. These components have traditionally been cast as single piece components. However, the recent trend is to cast smaller pieces which can be joined with sheet or forged parts in the fabrication of structural components as the turbine exhaust casing seen in figure 2 below².



Figure 2. A gas turbine hot structural part containing a large number of cast, sheet and wrought parts joined by welding.

The rationale for this fabrication strategy is the possibility to use higher strength wrought material, where geometry allows, and join these wrought parts with cast material where complex geometry is needed and the demand for strength is moderate. Since the assembly concept today is at the core of the VAC business the welding process is thus of the greatest concern³. This fabrication strategy enables a number of advantages such as the possibility to use more than one type of superalloy. An adequate superalloy part for a section with less stress or lower temperature is often less costly and can be joined with a more expensive but also more high performing one in an adjacent section as in the assembly part in figure 2 where small cast (“cheap”) Alloy 718 parts are joined with wrought (expensive) Alloy 718 parts by welding. Also, combinations of totally different alloys are possible e.g. Alloy 718 can be joined with the much more expensive Waspaloy, an alloy which can resist higher temperatures than Alloy 718. Furthermore, the costs associated with smaller cast parts in comparison with large cast parts are significantly reduced. One reason for this is that large cast parts most often suffer extensively from hot tears which subsequent need for repair. This repair is of course very time consuming and performed by manual welding.

A major challenge using the above strategy is the obvious fact that numerous of welds must be produced which requires the fundamental understanding of the alloys being joined by the specific welding processes.

1.2 Aim

As may be already understood, the requirements for more efficient aircraft engines have challenged researchers to develop new materials for these type of structural applications; materials which can operate at higher temperatures while preserving formability and especially good weldability. A comparison between the two widely used superalloys Alloy 718 and Waspaloy can here be made where Alloy 718 do possess good formability and weldability together with adequate high temperature strength up to ~650 °C while Waspaloy has better high temperature creep properties up to 750 °C but unfortunately associated with poor weldability and formability⁴. In this perspective the two new alloys Allvac[®] 718Plus[™] and Haynes[®] 282[®] developed by Allvac^{5, 6} and Haynes⁷, respectively, are of great interest since they both indicate improved high temperature performance over Alloy 718 and Waspaloy while keeping reasonable formability and welding characteristics^{5, 7, 8, 9, 10, 11 12, 13, 14}. All four alloys are compared from a weldability point of view in the present thesis work.

In order to solve welding problems which are encountered in present day manufacturing and to reduce anticipated ones it is necessary to understand what governs the weldability, not least in terms of cracking, from a generic, fundamental metallurgical point of view.

Heat treatments prior to welding, e.g., will alter the state of the material but at the same time influence the weldability. This concern is typical for the industrial practice but unfortunately very limited research results is available or at best contradicting^{15, 16} and different heat treatments are for this reason an integral part of the present research work. The understanding of the influence of secondary phases (e.g. carbides) in the

microstructure is in the present work addressed by systematic hot ductility testing (Gleeble) and by weldability testing (Varestraint). The effect of secondary phases are also analysed in practical welding as by electron beam (EB), and by gas tungsten arc welding (GTAW).

While modelling today impressively predicts distortions in the elaborate welding of complex structures as carried out at Volvo Aero the ability to predict the limits for the occurrence of cracking is still in its very infancy. The ultimate aim, where the work presented in this thesis is only a first step, is to have a modelling capacity which also can predict if cracking will occur or not. Weldability within this thesis is in this perspective defined as the ability on how a specific material is welded without experiencing any cracking. Response to post weld heat treatment while also important in this respect is not included except as an integral part of the multiple weld passes in the repair welding trials performed.

1.2.1 Objectives

The objectives of this research have been to investigate the weldability of precipitation hardened superalloys from a metallurgical standpoint. Two newly developed superalloys Allvac[®] 718Plus[™] and Haynes[®] 282[®] are compared with the two well established Alloy 718 and Waspaloy.

The research objectives on weldability:

1. The susceptibility towards cracking.
2. The effect of grain size on hot ductility and cracking.
3. The effect of secondary phase constituents on hot ductility and cracking.

Chapter 2

2 Aerospace Superalloys

Superalloys are as the name indicates alloys with superior properties at elevated temperatures and are based on nickel, nickel - iron or cobalt^{1, 17, 18}. They can be divided into three main groups based on strengthening mechanism; solid solution, precipitation and oxide dispersion strengthened alloys. These alloys are frequently used in high temperature and cryogenic applications in various fields such as aerospace/gas turbine, petrochemical and nuclear industries¹⁷.

In gas turbines there are very high temperatures in the combustor and subsequent turbine components exposed to high mechanical loads and thermal stresses¹. The high pressure turbine blades can be exposed to 1500 °C in the gas stream and on these critically hot parts cooling and thermally protective coatings are therefore applied to reduce the thermal load. Several types of contaminants from e.g. fuel combustion as well as by ingestion through the air stream like chlorides from sea water are also present^{1, 17, 18}. The temperature of the larger size structural weld assembly parts (figure 1 and 2) are however seldom allowed to exceed 800 °C¹⁸ and active cooling is not practical on these type of parts.

2.1 Manufacturing of Superalloys

Segregation of heavier elements to grain boundaries and interdendritic areas during the solidification is a well known phenomenon for all metallic alloys and especially for the superalloys with their complex chemistries. For critical applications, as in aircraft engines, the segregation and impurity is reduced and controlled through re-melting, first by vacuum induction melting (VIM) followed by vacuum arc re-melting (VAR) or electroslag re-melting (ESR). For the most critical applications as in disks there is usually a third VAR re-melting required¹⁹.

The control of the level of segregations at grain boundaries during melting and also the grain size during all subsequent processing steps are crucially important not only for the overall strength of an alloy but also for the fatigue and creep properties at higher temperatures which are very important properties in materials to be used in the turbine of aircraft engines^{1, 17, 18, 20}.

2.2 Physical Metallurgy of Superalloys

The chemical composition of the superalloys is very complex with many elements involved resulting in a number of secondary phases which all influence the specific alloy in one way or another. The base element of the alloys used in the present investigation is Ni or Ni-Fe. Some typically observed phases in wrought Ni-based superalloys are shown in table 1.

Table 1. Typically observed phases in wrought Ni-based superalloys¹⁷.

Phase	Crystal structure	Typical formula
γ	FCC	Ni (Cr, Fe, Mo)
γ'	FCC	$\text{Ni}_3(\text{Al, Ti})$
γ''	BCT	Ni_3Nb
δ	Orthorombic	Ni_3Nb
MC	FCC	TiC, NbC
M_{23}C_6	FCC	$\text{Cr}_{23}\text{C}_6, (\text{Cr, Fe, W, Mo})_{23}\text{C}_6$
M_6C	Cubic	$\text{Fe}_3\text{Mo}_3\text{C}$

The main reason for using Ni as a base element is mainly due to the ability to preserve high concentrations of alloying elements in solid solution, high thermal stability and an adequate cost. The alloying elements are added to improve properties such as; the oxidation and corrosion resistance, the strength and the high temperature stability. In table 2, the chemistries of Alloy 718, Allvac[®] 718Plus[™], Waspaloy and Haynes[®] 282[®] are shown. In the γ matrix secondary phases such as MC (metal carbide), MN (metal nitride), M_{23}C_6 , M_6C , γ' , γ'' , δ and Laves phases may be present.

Table 2. Chemical composition range in weight percent of Alloy 718²¹, Allvac[®] 718Plus[™]²², Waspaloy²³ and Haynes[®] 282[®]²⁴.

Element	Alloy 718	Allvac [®] 718Plus [™]	Waspaloy	Haynes [®] 282 [®]
Ni	50.0-55.0	Bal.	Bal.	Bal.
Cr	17.0-21.0	17-21	18.0-21.0	20
Fe	Bal.	8.0-10.0	2.0*	1.5*
Co	1.0*	8.0-10.0	12.0-15.0	10
Mo	2.8-3.3	2.5-3.1	3.5-5.0	8.5
Al	0.2-0.8	1.2-1.7	1.2-1.6	1.5
Ti	0.65-1.15	0.5-1.0	2.75-3.25	2.1
Nb	4.75-5.50	5.2-5.8	-	-
C	0.08*	0.01-0.05	0.02-0.1	0.06
P	0.015*	0.004-0.02	0.03*	-
B	0.006*	0.003-0.008	0.003-0.01	0.005
Cu	0.3*	-	0.5*	-
Mn	0.35*	0.35*	1.0*	0.3*
S	0.015*	-	0.003*	-
Si	0.35*	0.035*	0.75*	0.15*
W	-	0.008-1.4	-	-
Zr	-	-	0.02-0.12	-

*Max

2.2.1 The γ Matrix Phase

The austenitic γ phase constitutes the matrix phase with a face-centered cubic (FCC) structure. The matrix phase contains a wide range of alloying elements which provide solid solution strengthening to the alloy where Co, Cr, Fe, Mo and W (table 1) normally are used¹⁷.

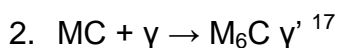
2.2.2 The Precipitation Strengthening Phases - γ' and γ''

The γ' and γ'' phases are the most important precipitation strengthening phases in the Ni and Ni-Fe based superalloys. The γ' phase is an FCC $\text{Ni}_3(\text{Al,Ti})$ phase whereas γ'' is a body centered tetragonal (BCT) Ni_3Nb phase^{17, 25, 26}. In both phases Co, Cr and Fe can substitute for Ni whereas Nb for Al and Ti¹⁷. The γ' phase has a low mismatch with the matrix which is associated with fast precipitation and a low coarsening rate. There is also solid solution strengthening of the γ' phase, primarily by partitioning of Nb. The γ'' phase on the other hand exhibits high coherency strains in the matrix due to a higher degree of mismatch with the matrix which confers higher strength but lower thermal stability and slower precipitation as compared with the γ' phase strengthening. Both the γ' and γ'' phases are metastable and can transform to the hexagonal close packed η and orthorhombic δ phases, respectively, if exposed to elevated temperatures for long times. The transformation from γ' to η phase is facilitated by increasing the Ti concentration but is not seen in the present alloys. The γ'' transforming to δ phase is on the other hand commonly seen in Alloy 718 and intentionally produced to improve certain properties such as stress rupture and also to control grain size since it pins the grain boundaries at elevated temperatures. Competing growth mechanism between the γ' and δ phases has been reported in the literature for Allvac[®] 718Plus^{™27}.

2.2.3 Carbides

There are many different types of carbides present in superalloys. The most commonly observed ones in the present alloys are the MC having a FCC crystal structure, the M_{23}C_6 and the M_6C with complex cubic structures^{1, 15, 17, 28, 29}. Furthermore, it is not unusual that $\text{M}(\text{CN})$ (metal carbo-nitride) form¹. The beneficial effect of the carbides is due to the strengthening affect at the grain boundaries. It has been shown that carbides inhibits grain-boundary sliding and hence improve creep and rupture strength^{1, 17}. It has also been shown that it is detrimental for the ductility and the rupture life when carbides are present as continuous chains at grain boundaries¹⁷.

Formation of carbides are initiated already in the liquid by the strong segregation of C and N. These two elements will then separately or jointly react with active elements such as Ti and or Nb which is often seen in Waspaloy, Alloy 718 and Allvac[®] 718Plus[™]^{17, 30}. At heat treatments and at service these MC carbides may decompose to other phases such as M_{23}C_6 at 760-980 °C and M_6C at 815-980 °C¹⁵, respectively, which are rich in Cr, Mo and W⁴. The most common reactions are:



The $M_{23}C_6$ and M_6C could also transform from one another¹⁷.

2.2.4 Other Phases

Other phases of interest belong to the previously mentioned incoherent and orthorhombic δ phase together with M_3B_2 boride and topologically close packed (TCP) phases.

The δ phase needles are thus incoherent with the matrix γ phase and do not confer any strength¹. It is generally accepted that extensive amounts of δ phase leads to loss of ductility^{1, 17}. The formation of δ phase takes place by a solid state diffusion mechanism between 650 and 980 °C in Alloy 718 and Allvac[®] 718Plus[™]^{1, 17, 27} but the phase is not present in Waspaloy or Haynes[®] 282[®]. The actual transformation mechanism differs depending on temperature; i.e. in Alloy 718 at temperatures below ~700 °C the growth occurs at the expense of γ'' phase whereas at temperatures between 700 and 885 °C the growth is facilitated by the rapid coarsening of the γ'' phase. At temperatures above 885 °C the γ'' is no longer stable and growth of δ phase takes place more rapidly to the solvus temperature of ~1000 °C¹. In Allvac[®] 718Plus[™] this is less clear since it is a γ' strengthened alloy. However, it has been shown that the same type of competing growth mechanism between γ' and δ phases takes place also here²⁷. The importance of having δ phase in the microstructure is related to its ability to pin the grain boundaries and consequently crucial for controlling the grain size. It has also been shown that it improves the stress-rupture properties^{17, 31, 32}.

B, as an important trace element, is generally present in levels up to ~50 ppm (table 2) but above ~60 ppm it severely affects the susceptibility to hot cracking and thus deteriorates the weldability^{15, 33, 34}. Boron and carbides both improve creep rupture strength^{1, 17}. The boride phase which has been observed is the M_3B_2 phase where M consists of elements as Mo, Ti and Cr^{1, 17}.

Undesirable TCP phases such as Laves, μ and σ may form as a consequence of long term service or heat treatment¹⁷. These phases are known to be very brittle^{17, 35}. The σ phase (rich in Cr, Ni and Fe) has been observed in Alloy 718 but is very rare³⁶. Laves phase, is another TCP phase with hexagonal closed packed structure and A_2B formula composition with Fe, Ni and Cr in the A position and Nb, Mo and Si in the B position¹⁵. It is commonly present in cast Alloy 718 and Allvac[®] 718Plus[™]^{17, 30} as a consequence of a strong segregation of the Nb during the solidification¹⁵.

2.3 Heat Treatments

During the manufacturing processes as forging, casting and welding many different kinds of heat treatments are carried out for annealing, homogenization and stress relieving⁴. Heat treatment for precipitation strengthening is usually carried out in two steps; a solution treatment followed by one or two aging treatments¹⁷.

The solution heat treatment is a high temperature treatment which is optimized to bring the age-strengthening phase into solution, i.e. a supersaturated solid solution of the alloying elements³⁷. If this treatment is carried out at sufficiently high temperatures secondary phases like δ phase (Alloy 718 and Allvac[®] 718Plus[™]) and certain carbides (Waspaloy and Haynes[®] 282[®]) are dissolved and grain growth will take place¹⁸. The solution treatment is the prerequisite for the later precipitation of the strengthening phase during the age heat treatment³⁷. This aging treatment can be monitored in steps in order to control the size and distribution of carbides (e.g. $M_{23}C_6$) and strengthening phases (e.g. γ' and γ'')¹⁸.

Chapter 3

3 Welding and Weldability of Aerospace Superalloys

By fusion welding different pieces of material are joined by a heat source capable of bringing enough heat/energy to melt the material at the junction and which differs with actual material, welding method and type of joint³⁸. It is possible to group welding processes based on their respective heat source i.e. gas flame (oxyacetylene welding), electric arc (gas tungsten arc welding (GTAW)) and high-energy beam (e.g. electron beam welding (EBW)). One important characteristic is the power density of the heat source. The power density and the costs related to the equipment increases significantly from the gas flame to the electric arc and the high-energy beam processes. The higher the power density of the specific weld process the less is the total heat input required to fuse the material which is beneficial from a distortion point of view. High density power processes therefore involves to less geometrical distortion, higher welding speed and deeper weld penetration³⁹. In the present work only GTAW and EBW have been used.

3.1 Gas Tungsten Arc Welding

GTAW is a process which uses a non-consumable tungsten electrode and suitable for welding thicknesses up to ~3 mm. This welding process can be carried out manually which is normally the case at repair work whereas automatic welding is the preferred choice in the production of aerospace components. Filler metal can be used and is either fed manually or automatically.

The actual heat generation is produced by an arc between the tungsten electrode and the workpiece. The tungsten electrode is placed inside a water-cooled copper tube to minimize the heating of the electrode. The copper tube is in turn connected to a power source which also is connected to the workpiece that closes the circuit. In order to protect the weld from oxidation an inert gas such as argon or a mixture of inert gases flows through a nozzle surrounding the electrode and over the workpiece³⁸.

Dependent on the type of material to be welded different polarity is used. For Ni-based superalloys a direct current electrode with negative polarity is preferred (connected to the negative side of the power source). The effect of this polarity is a more narrow and deep weld in comparison with a positive polarity or alternating current (AC)³⁹.

3.2 Electron Beam Welding

At EBW the parts that are to be joined are melted through the impact of a very dense electron beam. This is usually carried out in vacuum (10^{-3} to 10^{-6} torr) but could also be carried out at reduced-vacuum where the requirements on the weld quality are lower.

In the high vacuum electron gun the generation of electrons takes place at the cathode filament and are accelerated by an electric field together with the anode. The electrons

are focused by electromagnetic coils as they pass the small hole in the anode and finally directed onto a point at the work-piece.

The energy which is generated by the impact of the high energy electrons is often more than sufficient to vaporize the metal. This vaporization leads to a so called keyhole and very narrow welds which can be used to weld thicknesses up to ~300 mm in one weld pass³⁹.

There are two main types of EBW machines; low and high voltage machines operating at accelerating voltages (kV) and amperage (mA) in the intervals of 40 - 60 kV, 30 - 200 mA and 80 - 150 kV, 4 - 60 mA, respectively. The welding speed can be varied where low speed increase the risk of distortion while high speeds may enhance the risk of cracks and porosity^{39, 40, 41}.

Today there are many modes of manipulating the actual electron beam. Different focal points may be used; at surface, above surface or below surface. It is also possible to oscillate the beam in different modes at different frequencies i.e.; straight, circular, elliptical, triangular cycles or in other fashions. The workpiece angle and distance to the gun are additional welding parameters. It is also possible to use filler metal in EBW.

3.3 Residual Stresses in Welding

Geometrical distortion due to the stresses produced by the heating and cooling in the welding process is of major concern as are the different types of cracks produced for the same reason. Residual stresses and distortion are developed as a result of shrinkage and thermal contraction of the weld metal during the welding³⁹. The stress states are complex but have a longitudinal as well as a lateral component; the latter producing angular distortions³⁹. To avoid problems with the longitudinal stresses it is important to keep a symmetry of the welds with respect to component geometry. Rotational stresses are preferably minimized by having good weld bead symmetry with respect to the neutral axis of the component. This type of stress could also be lowered e.g. by pre-setting of the parts to be welded, proper joint preparation and weld pass sequence and/or by using a welding process such as EBW or laser beam welding which creates a weld bead with parallel sides. These high power density processes also reduce the overall distortion since their heat input is significantly lower compared with GTAW³⁹.

3.4 Weld Cracking

Weld cracking is a serious problem since it endangers component life which is the reason why non destructive testing (NDT) as X-ray and fluorescent penetrant inspection are always employed.

Cracking that can appear in a weld and in its surroundings, is schematically shown in figure 3 below. In the present thesis work focus is on the cracks which appear during the actual welding; in the heat affected zone (HAZ) by liquation and in the weld due to solidification shrinkage. If cracking occurs during the welding operation or during the

post weld heat treatment (PWHT) repair work is necessary. It goes without saying that there is a strong desire to eliminate all cracking by proper process control.

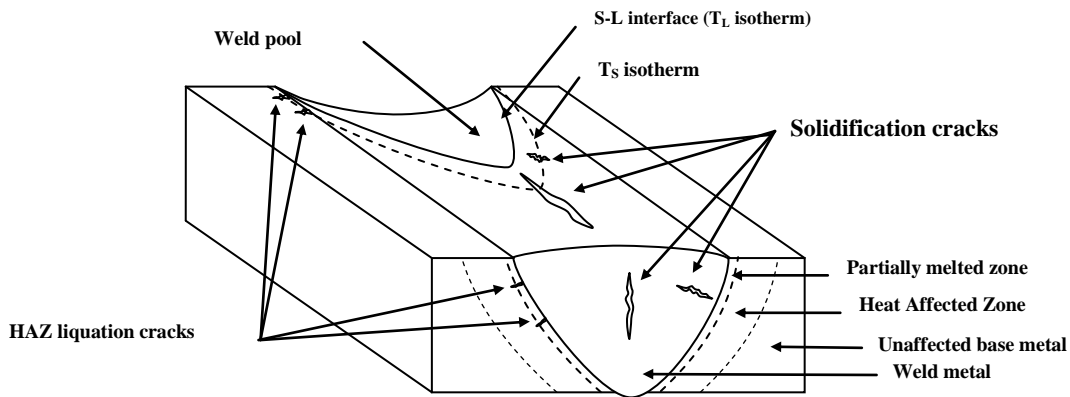


Figure 3. Schematic overview of weld cracking.

Cracking theories which are used in welding today emanates from the studies of solidification to describe hot tears during casting. A few of these theories are the “Strain theory of hot tears”⁴² and “Shrinkage-Brittleness theory”⁴³ which later were combined and modified by Borland to a theory known as the “Generalized theory”⁴⁴. All these solidification cracking theories are in different ways dependent on the presence of a liquid phase which together with thermally and mechanically induced strains enhances the susceptibility to cracking. The theories were initially adapted to fusion zone solidification cracking in welding but later also to HAZ liquation cracking.

There are different ways of grouping cracks. Hot cracking is a group of cracks which includes those cracks which are associated with a liquid and are located in the fusion zone (FZ) and the partially melted zone (PMZ) of the HAZ as indicated in figure 3 above. Warm cracking is another group of cracks which occurs in the FZ and HAZ at elevated temperature but is not associated with any liquid. Cold cracking can occur at low temperatures (near room temperature) and is usually induced by embrittling species such as hydrogen¹⁵.

In the following an in depth description of solidification, HAZ liquation and strain age cracking (SAC) is made since these cracking phenomena are of the highest importance in the welding of Ni-based superalloys.

3.4.1 Solidification Cracking

In the early 1950s Pellini proposed the **strain theory**⁴² relating to the formation of a continuous liquid film which separates the solidifying metal. The strength and ductility of these solid grains separated by a continuous liquid film is very low and was accepted as the “Film stage”⁴². As thermal contraction and shrinkage stresses increase appreciably near the solidus temperature, this film stage causes intergranular rupture. The time, temperature and the ability of the liquid phase to spread along the grain boundaries to form a semi or continuous liquid film affect the susceptibility to liquation cracking.

The **shrinkage-brittleness theory** on the other hand recognizes the inability of the newly formed dendrites to accommodate strain⁴³. Pellini (“Film stage”) on the contrary proposed that the stresses that are formed in the mushy zone are uniformly distributed and postulated that cracking cannot occur at this stage. However, in the shrinkage-brittleness theory it is suggested that the temperature range at which cracking occurs is between the solidus and the coherency temperature which is the temperature at which the dendrites meet for the first time. If a certain critical strain is exceeded within this temperature range, recognized as the brittle temperature range (BTR) and if no liquid phase is present to heal, a hot tear would appear⁴³. The BTR is highly dependent on alloy composition which means that alloys possessing a wider solidification range are more prone to solidification cracking.

Later Borland proposed a new **generalized theory** based and modified on some of the previous theories⁴⁴. He divided the solidification sequence at welding into four different stages:

- Stage 1. Primary dendrite formation, where movement of both solid and liquid phases is significant.
- Stage 2. Dendrite interlocking (coherency temperature), involves the development of continuous formation of both solid and liquid phases. However, it is only the liquid which is able to move freely between the interlocking dendrites.
- Stage 3. Grain boundary development (the critical temperature), where the semi-continuous network of dendrites restricts free movement of the liquid phase.
- Stage 4. Solidification, where the final liquid phase solidifies.

According to Borland a crack can possibly appear as temperature drops below the coherency temperature and is more specifically related to the so called “critical solidification range” (CSR) which belongs to stage 3 where the interlocking mechanism of dendrites restrict liquid phase movements, hence, relative movement and healing is hindered. The susceptibility to liquation cracking is enhanced as the CSR is increased. Further, Borland emphasize the importance of the relationship between the ratio of the interphase (solid/liquid) boundary tension (γ_{SL}) and grain boundary tension (γ_{SS}) to the dihedral angle (distribution of liquid phase on grain corners, edges and faces). When the dihedral angle is 0° it ($\gamma_{SL}/\gamma_{SS} = 0.5$) means that the liquid phase completely penetrates the existing grain boundaries leading to complete de-cohesion between the adjacent grains. However, the stresses are very low which leads to low cracking susceptibility. As the dihedral angle is increased the liquid phase will progressively occupy less of the grain faces and at an angle of 60° it will only exist as continuous network along grain edges. At even higher angles the liquid phase will be more and more limited to grain corners. Dihedral angles slightly above 0° will lead to small bridges of the dendrites, hence, building up high stresses which lead to high susceptibility to

cracking. At higher dihedral angles more bridging will take place and reduce the susceptibility to cracking⁴⁴.

There are many other hot tearing theories proposed in addition to the ones previously presented^{45, 46, 47, 48}. The metallurgical factors which have been known to affect the solidification cracking susceptibility can nevertheless be summarized in the following way³⁹:

1. The solidification temperature range.
2. The amount and distribution of liquid at the final stage of solidification.
3. The primary solidification mode.
4. The surface tension of the grain boundary liquid.
5. The grain structure.

Segregation is of prime concern in superalloys. It is due to the inevitable partitioning of the many chemical elements involved in these alloys. How extensive the segregation becomes is dependent on the so called partitioning coefficient k , defined as the ratio of the concentration of the solute in the solid to that of the liquid in equilibrium⁴⁹.

$$k = X_S/X_L \quad (1)$$

Where, X_S and X_L are mole fractions of solute in the solid and liquid phases, respectively, at a certain temperature. If the partitioning value is less than unity the element tend to segregate into the interdendritic region whereas if it is greater than unity it is enriched in the dendritic core region. The following elements are example of elements which are enriched between the dendrites: S, O, B, P, C, Ti, N, H and Nb⁴⁹. The characteristic feature of these elements is that they all depress the melting point and consequently take part in eutectic phase reactions to produce wetting films at the grain boundaries which significantly weakens the material⁵⁰.

Solidification cracking of austenitic materials is strongly dependent on the solidification temperature range and in particular the solidification events at the grain boundaries and interdendritic regions^{51, 52 53}. Particularly this has been shown to be true for alloys containing Nb which promotes the formation of NbC and Laves-phase eutectics at the very final stages of solidification^{54, 55, 56, 57, 58, 59, 60, 61, 62}. The Laves eutectic is known to be more detrimental than the MC eutectic since it solidifies at a lower temperature and as such extends the solidification temperature range^{54, 63} (**paper I and II**). The amount of these two phases is highly dependent on the nominal alloy composition^{54, 64}. Studies by Dupont et al. have shown that by varying the amount of C it is possible to eliminate the $\gamma + \text{Laves}$ eutectic reaction which may reduce the susceptibility to solidification cracking¹⁵. The C/Nb ratio affects the amount and distribution of the $\gamma + \text{NbC}$ eutectic and $\gamma + \text{Laves}$ eutectic which influence the effective solidification temperature range and

with a continuous eutectic network being worse than an isolated network of eutectic constituents¹⁵. However, it should be noted that eutectic constituents may reduce cracking through backfilling^{30, 65, 66, 67} (**paper V**).

With regard to grain structure morphology it is generally claimed that an equiaxed structure is less susceptible to solidification cracking than one with a columnar structure³⁹. This advantage is attributed to the better accommodation of strain, liquid feeding, healing of incipient cracks and to the lower concentration of impurity elements of equiaxed grains^{39, 68}.

3.4.2 Heat Affected Zone Liquation Cracking

It is generally accepted that HAZ liquation cracking in precipitation hardened superalloys is due to stresses developed by shrinkage during solidification and cooling in association with re-precipitation of secondary phases such as γ' phase during the cooling. Liquation of grain boundary constituents reduces ductility to zero and consequently also very moderate stresses will cause cracking.

Cracking can be prevented by minimizing the heat input through the choice of a high energy welding process to reduce the thermally induced stresses which may be the first option and while a second could be to weld the material in the most suitable heat treatment condition^{15, 39}.

Research on superalloys (especially on Nb bearing alloys) has shown that it is the liquation of grain boundaries which determines how susceptible a material will be to HAZ liquation cracking¹⁵. There are different explanations to how liquation takes place in the PMZ of HAZ of a material and which are summarized in the table below³⁹. These explanations are somewhat adaptable for alloys like Alloy 718 and Allvac[®] 718Plus[™] with reference to the symbols in figure 4 below (**Paper V**).

1. Melting of the matrix.
2. A hypothetically superalloy composition with a ($C_{Nb} > C_m$) Laves phase reacting with the matrix ($\gamma + \text{Laves} \rightarrow \text{Liquid}$).
3. Melting of a hypothetically superalloy composition ($C_{Nb} > C_m$) with a eutectic microstructure constituent ($\gamma + (\gamma + \text{Laves}) \rightarrow \text{Liquid}$).
4. Constitutional liquation of secondary phases such as Ni_2Nb (Laves) and NbC or NbC phase in cast and wrought Alloy 718, respectively¹⁵ (**Paper V-VII**).
5. Melting of residual eutectic in cast material¹⁵ (**Paper IV**).
6. Segregation induced liquation by grain boundary sweeping mechanism leading to accumulation of solutes like B and S at the migrated grain boundaries³⁹ (**Paper VIII**).

The above mechanisms are highly influenced by the pre-weld microstructure in the HAZ and on which the modified pseudo binary phase diagram in figure 4 (**paper V**) may shed some light.

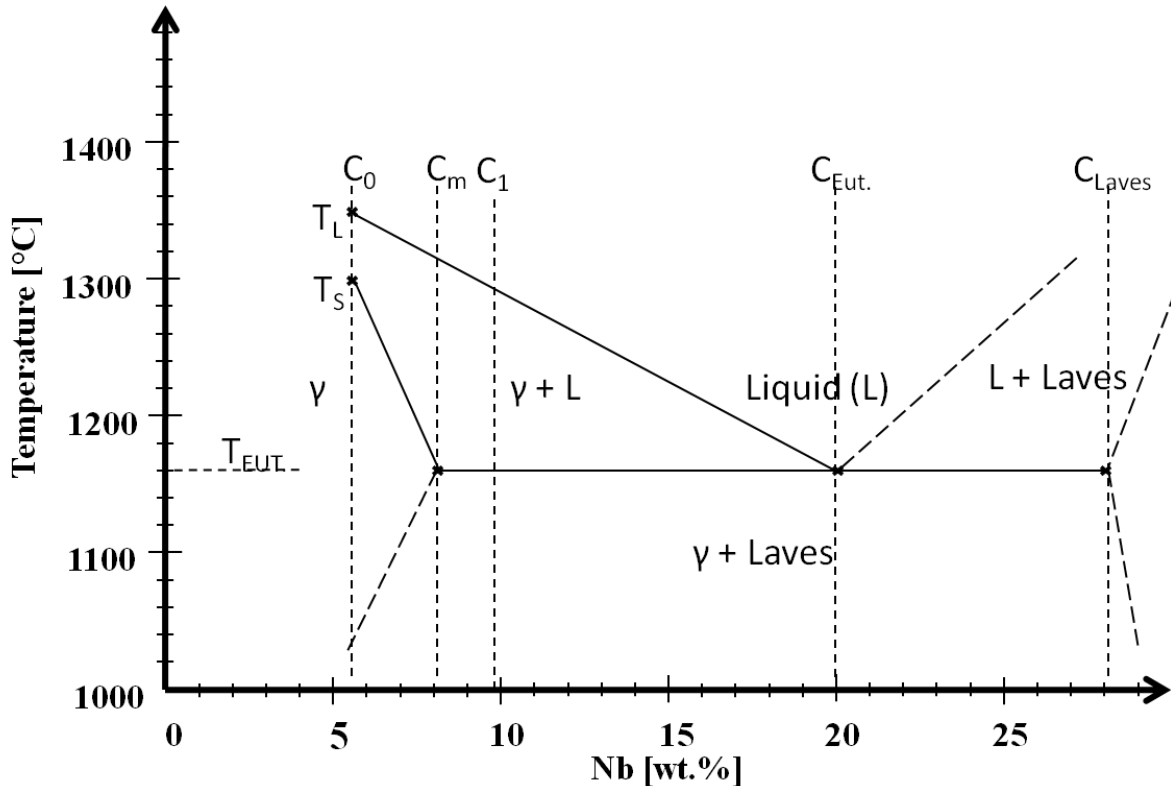


Figure 4. Pseudo binary phase diagram of Allvac® 718Plus™ superalloy, adapted from paper V.

In the pseudo binary phase diagram in figure 4 it can be seen that three phases co-exist at the eutectic temperature (T_{EUT}); γ , Laves and Liquid (L) phases. It should be noted that a diagram of this type is a simplification of e.g. Alloy 718 or Allvac® 718Plus™ system. C_0 is the nominal composition of Nb both in Alloy 718 and Allvac® 718Plus™ whereas the C_1 corresponds to a nominal alloy composition of Nb which exceeds the maximum solubility of Nb within the γ phase and therefore not applicable to either Alloy 718 or Allvac® 718Plus™. The C_m and C_{Laves} are the maximum solubility of Nb in the γ phase (~8 wt% Nb) and the composition of the Laves phase, respectively. T_S and T_L are the solidus and liquidus temperatures of the γ phase at composition C_0 .

For the liquation according to the mechanism, $\gamma \rightarrow L$ at T_S , (number 1 on the list) to occur the alloy must have an Nb concentration below C_m . Furthermore, no Laves phase or any other secondary phase should be present within the austenitic matrix to avoid liquation at T_E . This reaction is highly dependent on the heating rate, presence and amount of secondary phases. Both Alloy 718 and Allvac® 718Plus™ contain other phase constituents with high Nb content such as NbC and δ which may participate in

melt reactions and which has been thoroughly investigated in the present thesis work^{15, 17, 30, 69}.

Mechanism number two (**Laves + γ → L at T_E**) requires an austenitic γ matrix together with Laves phase particles and a nominal composition (C_1) higher than C_m . This mechanism occurs regardless of heating rate. This reaction is not applicable to Alloy 718 or Allvac[®] 718Plus[™] since the Laves phase is not thermodynamically stable at the homogenized nominal composition C_0 .

At the third mechanism which involves a eutectic structure (hypoeutectic) at a composition higher than C_m includes a γ matrix and eutectic constituents (**$\gamma + (\gamma + \text{Laves}) \rightarrow L$**). This reaction is as well as reaction number two independent of heating rate. It does not take place in the present alloys since the nominal alloy composition (C_1) is too high meaning that the $\gamma + \text{Laves}$ eutectic constituent is not stable from equilibrium point of view at a nominal alloy composition of C_0 and may be dissolved given enough time below the T_E temperature (as performed at homogenization treatment of cast components).

The eutectic reaction number four (**Laves + $\gamma \rightarrow L$ at T_E**) still occurs during welding in Alloy 718 or Allvac[®] 718Plus[™] due to the presence of the thermodynamically stable phase constituents with high Nb content as carbides and δ phase in the wrought material although no Laves phase is present and has been the subject for research for many years. This phenomenon is named constitutional liquation and was explained in general terms by Pepe and Savage⁷⁰ and later for Alloy 718 by Owczarski et al⁷¹. The reaction takes place at the interface between the matrix (at nominal composition C_0) and the secondary phase with a high Nb content (NbC or δ) provided these secondary phases survive the heating up to T_E without being dissolved through solid state diffusion^{72, 73}. For the δ phase this is disputable since it generally dissolves at much lower temperatures while for NbC the reaction is more expected due to the much higher solution temperature. In the present thesis work constitutional liquation not least of the δ phase in both Alloy 718 and Allvac[®] 718Plus[™] is treated in depth (**paper V**).

The last liquation mechanism (**Residual eutectic (Laves + γ) → L at T_E**) is only expected in cast materials. Since nominal composition C_0 is below C_m the reaction can theoretically be avoided if the material is given enough time for homogenization which will finally dissolve the eutectic. In welding of cast material the reaction is however not possible to avoid due to the rapid heating.

Reaction number six involves segregation of minor elements such as B^{33, 34, 74, 75, 76, 77}, P^{78, 79}, S^{80, 81} and C^{74, 82} to the grain boundaries where they aid liquation during the on heating weld thermal cycle through depressing the melting point temperature and also extending the solidification temperature range on cooling^{83, 84}. This problem may be aggravated when grain boundary migration takes place when boundaries “wash” the material clean and these trace elements accumulates at the grain boundaries by the sweeping action³⁹. Pipe diffusion from the FZ grain boundaries to the PMZ³⁹ may have a similar effect.

It is possible to influence the above liquation mechanisms by heat treatments as those carried out in this study and reported in papers VI-IX. It is though not unusual to find conflicting result in literature with regard to what heat treatment may be the most favorable¹⁵. Nevertheless, it is generally claimed that a material in the softest possible solution heat treated condition together with fine grains is to be preferred to the same material in a coarse grain and aged, hard condition in terms of the susceptibility to HAZ liquation cracking^{15, 68}. The benefits with regard to the grain size are attributed to a better ability of small grain to accommodate the strains developed during the weld thermal cycle³⁹. The larger total grain boundary area of a small grain material compared with a large grain material will better accommodate the strain and will also reduce the stress concentration at the grain boundary triple points which are the most susceptible to crack initiation¹⁵. Also, the grain size can influence the thickness of the liquid film which develops during welding, hence, smaller grains result in thinner films⁸⁵. As grain size increases the concentration of e.g. B, P and S will also increase and impose a damaging effect as explained in the above liquation mechanism (number six)⁶⁸.

Regarding the secondary phases present in Alloy 718 and their influence on HAZ liquation cracking it has been shown that it is attributed to the constitutional liquation of NbC⁸⁶ in wrought form and to NbC together with Laves in cast form^{87, 88}. For the δ phase it has been claimed that it improves cracking resistance through a “solute blocking mechanism” (reducing the amount of free Nb)⁸⁹ while others have found it to increase the susceptibility to liquation cracking by assisting liquation^{90, 91}. Grain boundary segregation of minor elements like B, P, C and S seem to enhance HAZ liquation cracking in both Alloy 718 and Waspaloy^{15, 92}. HAZ liquation in Waspaloy has been suggested to occur by the segregation of minor elements like B⁹³ and also through “pipeline” diffusion of Al and Ti from the FZ to the HAZ⁹⁴ and by constitutional liquation of TiC phase⁷⁴. Regarding Allvac[®] 718Plus[™] research performed is however limited. Krutika showed that both large grain size and high B and P levels in a modified Allvac[®] 718Plus[™] alloy have an impact on the cracking response³⁰. The same study also explained that cracking in Waspaloy was due to the extensive precipitation of inter- and intra-granular γ' .

3.4.3 Strain Age Cracking

SAC is a type of cracking that occurs in the solid state due to hardening in the material when weld stresses are high at the same time and occurs in precipitation hardened superalloys and in γ' strengthened alloys in particular. In general, SAC takes place during the PWHT why it sometimes is referred to as “PWHT cracking” or “Reheat cracking”¹⁵. However, it may also occur during multipass welding, e.g. repair welds as was evident as was reported in **paper IX**. SAC is the biggest concern when welding γ' strengthened Ni-base superalloys and was actually a strong reason for the success of Alloy 718 since there was a large demand for a high temperature capable alloy which was readily weldable. Alloy 718 is more or less immune to SAC due to its sluggish strengthening response of γ' phase.

The reasons for performing a solution heat treatment (PWHT) after welding is not only to restore the microstructure of the FZ and HAZ but also to relieve the stresses which build up during the welding operation¹⁵. Unfortunately most of the stress relieve seem to occur concomitant with the precipitation hardening during the heating cycle of PWHT which impose high strain on the grain boundaries. Also the hardening of the alloy generally leads to a reduced overall ductility⁹⁵. Due to this loss of ductility, ductility dip cracking (DDC) may occur. DDC is another type of cracking more common in other alloy systems (e.g. solid solution strengthened alloys) where it is thus not related to precipitation hardening¹⁵. The ductility drop is presumably associated with severe strain concentration at grain boundary triple points due to grain boundary sliding¹⁵. Research has shown the beneficial effects of carbide precipitation (e.g. $M_{23}C_6$ and MC) in resisting grain boundary sliding and decohesion at elevated temperatures¹⁵. According to Lippold et al. it is this beneficial effect by the precipitation of MC carbides which hinders grain boundary migration, hence, creates tortuous grain boundaries by pinning⁹⁶.

Regarding SAC several more factors than those mentioned above may increase the susceptibility. The relation between Al and Ti was proposed by Prager and Shirra who suggested a strong influence on the precipitation characteristics of the γ' and basically the higher the content of these hardening elements the more susceptible the alloy will be⁹⁷. Carbide films at the grain boundaries together with grain boundaries partially liquated during the weld cycle are also reported to contribute negatively⁹⁸. These material specific factors together with the stresses developed by the welding operation add to the severity of the cracking susceptibility¹⁵.

3.5 Weldability Testing

There are hundreds of weldability testing methods⁹⁹ where the term weldability often refers to the “inherent” resistance to cracking in a material during welding and this definition is also used throughout the present thesis. It should however be noted that the term weldability may also incorporate the quality of the weld from a service performance point of view^{15, 39}.

There is no single testing method which can be used to study all parameters relating to cracking and/or service performance of welds. Every method has its specific character. The hot/warm cracking tests can though be grouped into different categories such as the representative tests, the simulative tests and the high temperature mechanical tests¹⁰⁰. Only the methods used in this thesis work, the Gleeble method and the Varestraint method will be presented in this summary. These testing methods are also among the most commonly used ones when evaluating hot cracking susceptibility¹⁵.

It should be emphasized that there is no “hot cracking” test which have been properly standardized and large variations in the actual setup of the testing are evident although the name of the test is the same¹⁰¹. A round robin study performed with the Varestraint testing method to evaluate the “weldability” of a number of superalloys at a number of test sites produced disappointing results with no two laboratories having even the same rating of the weldability (amount of cracking)¹⁶. This was attributed to the lack of standardization, in terms of procedures and equipment.

Often it is difficult to separate what kind of cracking – HAZ liquation cracking or solidification cracking – has occurred. Also the way to enumerate the cracking differs which make direct comparison of little value and care should therefore be taken when interpreting test results from different laboratories or should maybe to be avoided completely. However, the use of simple metallographic examinations of welds often provides very good information in terms of material behavior and to gain insight in the cracking mechanisms¹⁰². Testing methods are still of value when a specific cracking mechanism is investigated. It also provides a way of developing different cracking criteria which can be used to predict cracking.

3.5.1 Representative Tests

There are many different kinds of representative tests e.g.: Circular patch test, Lehigh test, Keyhole test (including the slotted test) and the Houldcroft tests to mention only three¹⁰³. These tests are used without any application of external loads and believed to be representative of actual welding situations but designed to reflect different degrees of constraint¹⁵. Repair welding tests are commonly used where a certain groove is designed, machined and repaired to reflect a real repair situation of a component. This was performed in the present work as reported in paper IV and IX. The main drawback regarding these tests is that it is not possible to quantify the amount of restraint during welding and the tests simply provide information whether the material has cracked or not without any detailed information about the limits¹⁵. Metallography, usually performed, still adds to the understanding of mechanisms.

3.5.2 Gleeble Hot Ductility Test

The Gleeble test was developed in the welding research laboratory at Rensselaer Polytechnic Institute in 1949 by Nippes and Savage¹⁰⁴. The name “Gleeble” is according to Lundin attributed to the predilection of a graduate student who used to give names to various pieces of equipment¹⁰⁵.

The Gleeble testing system uses resistance heating for the heating of a small test specimen according to a preprogrammed temperature cycle and monitored through percussion welded thermocouples in a closed circuit loop. At a selected temperature and strain rate tensile testing is performed and the reduction of area (RA) is later measured and used as a means to evaluate the hot ductility. The temperature cycle may e.g. reproduce a weld HAZ temperature cycle close to the FZ boundary¹⁰⁶.

The 1500D Gleeble testing machine used in the present work is shown in figure 5 below together with a test setup. The specimen is fixed by a water cooled copper grip at each end enabling the current to pass through the specimen for the heating. This equipment also furnished a water quenching device for extreme cooling rates.

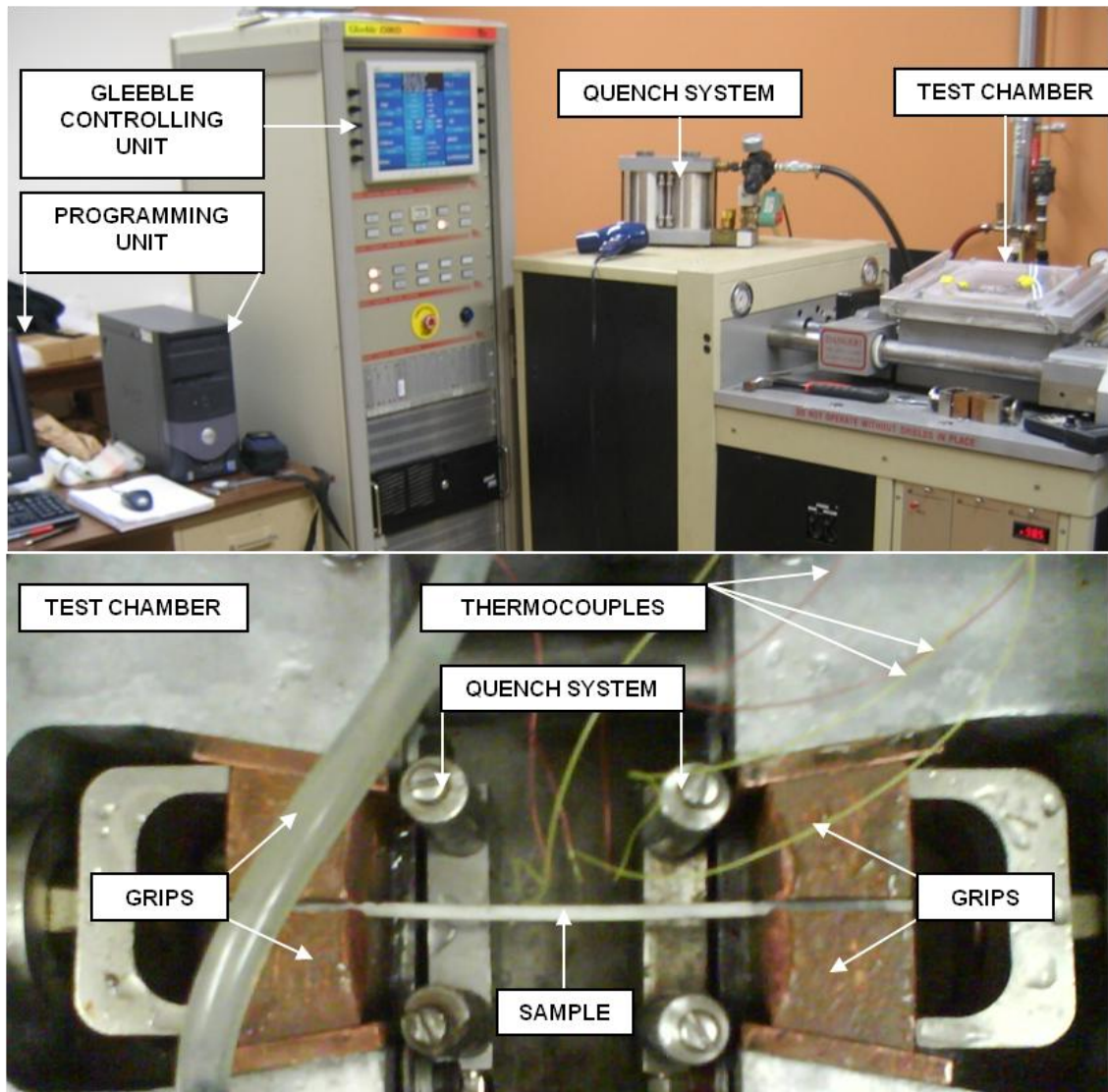
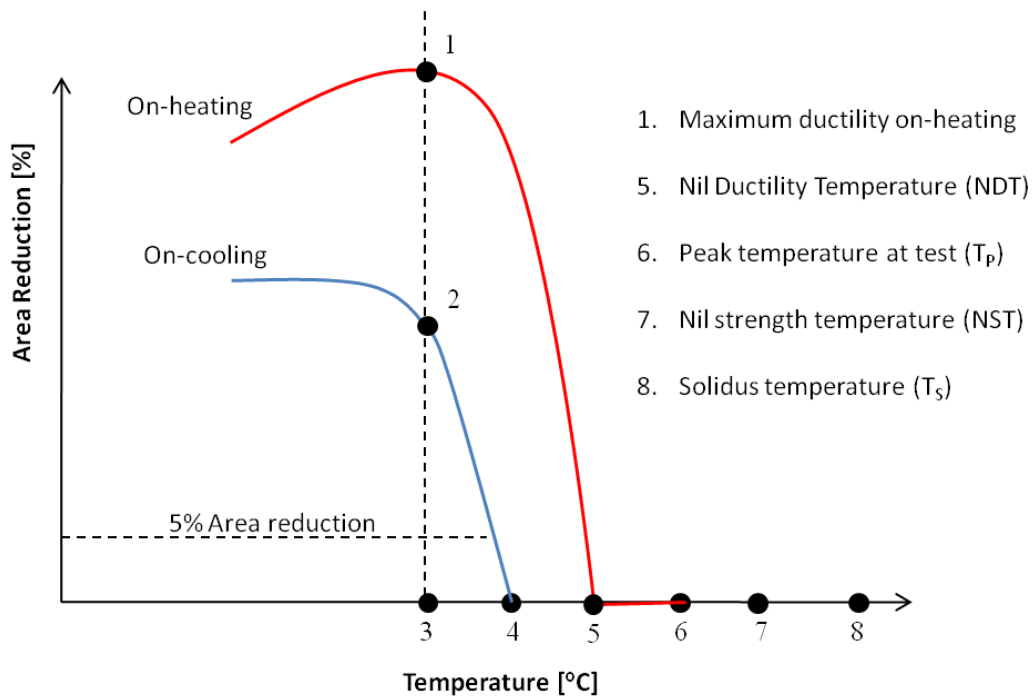


Figure 5. A 1500D Gleeble testing machine at University of Manitoba.

With this type of testing it is possible to produce ductility temperature curves to understand where the material becomes brittle on-heating but also when ductility recovers on-cooling¹⁵. The characterization of a material's hot ductility based on Gleeble testing mainly consists in determining the nil ductility temperature (NDT), nil strength temperature (NST) and ductility recovery temperature (DRT) as schematically shown in figure 6 together with ductility weldability parameters. In the on-heating thermal cycle in figure 6 the maximum ductility point is followed by a fairly abrupt decrease in ductility which is due to the onset of liquation¹⁵. The NDT point corresponds to a temperature where the ductility is virtually zero. At NST the material exhibits zero strength. The NST minus 30 °C is commonly used as the peak temperature (T_P) in the on-cooling tests for Ni-base superalloys which tend to suffer from severe liquation¹⁵. At the on-cooling thermal test cycle the DRT parameter is the temperature where the material ductility has recovered with 5 % RA¹⁰⁷. The DRT reflects the temperature that represents a point

where the liquid in grain boundaries at T_p has solidified and significant ductility is present¹⁵. As may be anticipated there are different ways of interpreting hot ductility curves and to measure the susceptibility to hot cracking in a welding situation^{106, 108}.

Three different measures are presented in figure 6; the brittle temperature range (BTR) which is the difference between T_p and DRT, ductility recovery rate (DRR) being determined at a specific temperature from the on-heating and the on-cooling hot ductility curves as the ratio of percentage RA, and finally the ratio of ductility recovery (RDR) which is calculated by determining the ratio of the areas under the on-cooling and on-heating hot ductility curves^{107, 109}.



Ductility Recovery Temperature (DRT): The temperature where 5% area reduction on-cooling is measured.

Brittle Temperature Range (BTR): T_p -DRT

Ductility Recovery Rate (DRR): $(2-3)/(1-3) \times 100$

Ratio of Ductility Recovery (RDR): $\text{area}(2-3-4)/\text{area}(1-3-5) \times 100$

Figure 6. A schematic and typical hot ductility signature together with weldability parameters.

These weldability parameters (BTR, DRR and RDR) are all associated with the formation of grain boundary liquation. Here the BTR and RDR reflects the hot ductility

response over a temperature range while the DRR parameter only reflects the ductility situation at one specific temperature¹⁰⁷.

Regarding the actual testing parameters Lundin et al. elaborated on six different areas of great concern for the Gleeble testing method which are listed below together with the recommended conditions and procedures in table 3¹¹⁰:

1. Thermocouple attachment technique.
2. Thermal cycle.
3. Peak temperature (for on-cooling tests).
4. Crosshead speed (strain rate).
5. Hold time at test temperature.
6. Testing procedure.

Table 3. Summary of Gleeble hot ductility testing conditions and procedures as suggested by Lundin et al¹¹⁰.

Parameter	Conditions
Sample	Diameter: 6.35 ± 0.025 mm; cylindrical; length 102 ± 3 mm; thread ¼-20 on both ends.
Thermocouple	Diameter: 0.254 mm; Chromel-alumel: < 1371 °C, Noble Metal/Alloy: > 1371 °C. Attachment methods: Percussion/Spot Welding, Separate Wire Technique.
Thermal Cycle	Characteristics of a SMAW weld in 38 mm thick stainless steel with an energy input of 2.8 KJ/mm at 22°C preheat.
On Cooling Peak Temperature	Nil ductility or nil strength temperature.
Hold Time	Test temperature: 1-2 seconds permitted. Peak temperature: Not permitted.
Crosshead Speed	63.5 ± 13 mm/sec.
Jaw Separation	20 ± 5 mm.
Testing	Minimum of 2 tests at each temperature. A difference of greater than 30 % in reduction in area, will necessitate one more test. Testing Temperature Intervals : 56-111 °C intervals below NDT-56 °C or NST-56 °C; 14 °C intervals between NDT and NST.

Gleeble parameters suggested as the “best practices” at the Welding Metallurgy Laboratory at The Ohio State University are summarized in table 4¹⁵:

Table 4. Summary of Gleeble testing “best practices” at the Welding Metallurgy Laboratory at The Ohio State University¹⁵.

Parameter	Conditions
Sample	Same as Lundin.
Jaw Separation	25 mm.
Determining the NST	Determined by heating at linear rate 111 °C/s under static load of 10 kg until sample failure.
Thermal Cycle	All tests should run in Argon. On-heating tests are conducted by heating to the specific test temperature at a rate of 111 °C/s and then pulling to fracture. On-cooling tests are performed after heating the sample to the NST or somewhere in between NST and NDT point at 111 °C/s and then cooling to the test temperature at 50 °C/s and pulled to fracture.
Crosshead Speed	50 mm/sec.

There is no standardized way of performing Gleeble hot ductility testing why differences between laboratories definitely exist. Also, it is not possible to directly compare the weldability predictions obtained by Gleeble testing with results from high power density processes such as Laser and EB welding since the cooling rates in Gleeble testing are much lower³⁹. Another discrepancy is that the surface temperature of the Gleeble specimen is lower compared to the inner part of the specimen. Furthermore, the temperature gradient throughout the specimen is much lower compared to weld HAZ which may result in a different microstructure in comparison³⁹. Another lack of conformance is that crack healing by backfilling, which occurs in welding, is very far from being reflected by the Gleeble testing.

3.5.3 The Vareststraint Test and Derivatives

In 1965, a few years after the development of the Gleeble test another hot cracking test known as the Vareststraint test (**V**ARIABLE **RE**STRAINT) was developed by Savage and Lundin at the Rensselaer Polytechnic Institute¹¹¹. This method made it possible to study hot cracking susceptibility by a systematic procedure reflecting the real weld situation, that is; small and simple specimens could be used to study the influence of the material, the welding process and not least the constraint factors on the hot cracking behaviour (HAZ liquation cracks and solidification cracks). The idea is to rapidly apply an augmented strain during the welding of a plate as seen schematically in figure 7. The amount of augmented strain (ϵ) depends on material thickness and radius of the die block according to the following equation:

$$\epsilon = t / 2R \quad (2)$$

where t is the specimen thickness and R the radius of curvature of the die block. This procedure provided a way to simulate the effect of large strains associated with highly restrained production welds¹¹¹. The augmented strain is simply altered by changing the die block radius.

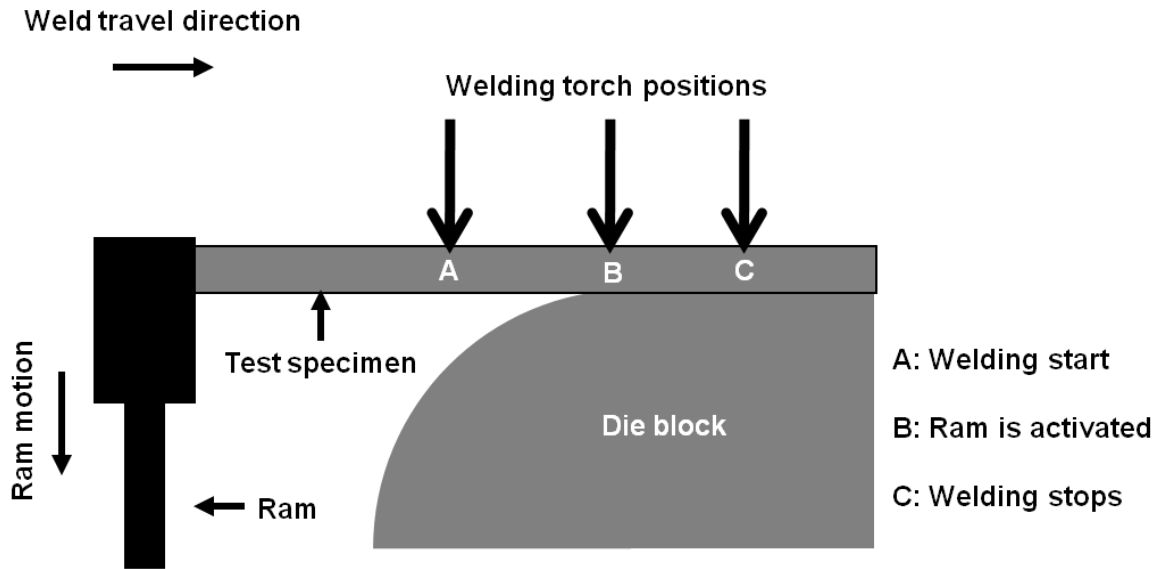


Figure 7. A schematic view of the Varestraint test.

In figure 7 the Longitudinal Varestraint is shown but there is also a Transvarestraint, a Spot Varestraint (or TIG-A-MA-JIG) as well as a sub-scale Varestraint test¹¹². As the names indicate the difference between the Varestraint test methods is the way to geometrically apply the weld gun during the straining as shown schematically in figure 8. The transverse test is used to study solidification cracking whereas the spot test is used for evaluating the HAZ liquation cracking susceptibility¹¹².

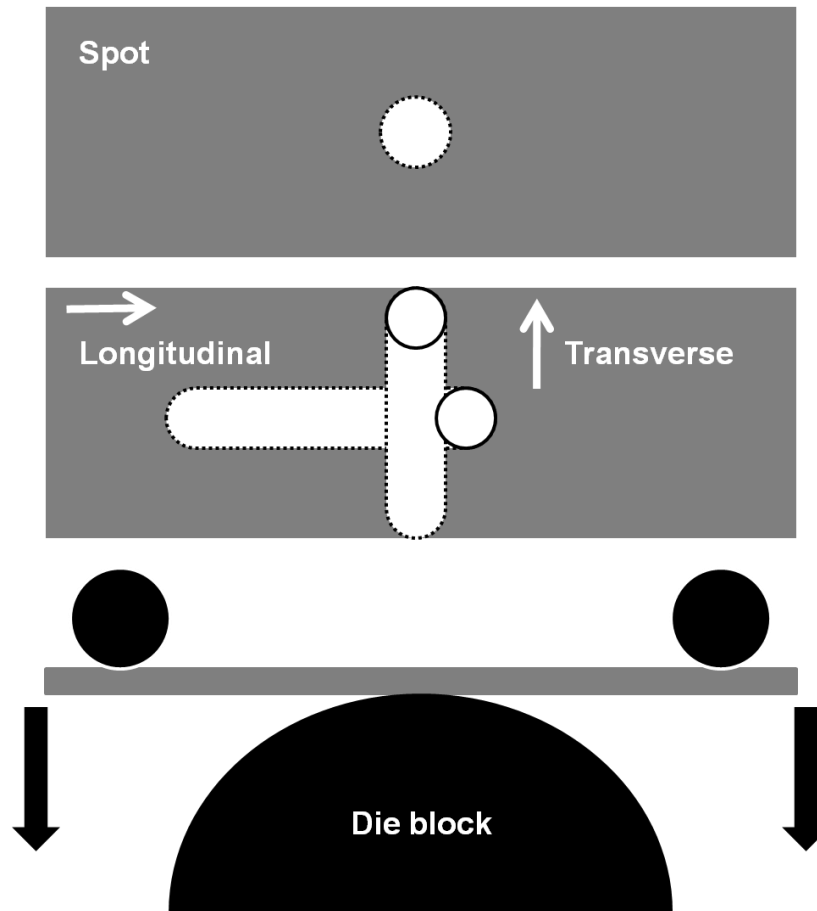


Figure 8. Schematic view of the Longitudinal Varestreint, Transvarestreint and Spot Varestreint tests. Figure is adapted from Dupont et al¹⁵.

It is also possible to evaluate filler metals. Some testing facilities use a slow bending test procedure with higher demands on the synchronization of the torch to maintain the work-piece distance¹⁵.

Different approaches are used to evaluate the Varestreint test results. First the as-welded surface is examined for cracking usually by means of a stereo microscope at a low magnification (20-60X magnification)^{15, 112}. If it is hard to distinguish the cracks the samples can be slightly etch or subjected to limited cold strain prior to the examination¹¹². The following evaluation procedures are the commonly used in the Varestreint testing.

- Total crack length (TCL): The length of all cracks either the HAZ or FZ are summarized for comparison¹¹².
- The maximum crack length or the maximum crack distance (MCL or MCD) reflecting the brittle temperature range (BTR) or the solidification cracking temperature range (SCTR)^{15, 112}.

- The cracking threshold strain (CTS) corresponding to the minimum amount of augmented strain needed to cause cracking¹¹².
- Saturated strain which represents the augmented strain above which the MCD do not increase¹⁵.

The MCL/MCD and TCL are commonly plotted against the augmented strain. It is recommended that three specimens are tested under the same conditions¹¹².

Lundin et al. suggested the travel speed, amperage and test thickness to be the three most important variables to control the cracking response at Varestraint testing assuming that electrode size and geometry, inert gas flow, electrode extension and arc gap are all held constant¹¹². These variables seemed to be important since cracking was postulated to propagate readily over a cracking temperature range and consequently highly dependent on the temperature gradient. Decreasing the thermal gradient increases the cracking susceptible region and would therefore result in an increased amount of cracking¹¹². When they separately looked at the influence on amperage, specimen thickness and the weld travel speed on the cracking susceptibility they concluded that both TCL and CTS increased when the current increased from 150 to 230 amps and as specimen thickness decreased from 0.325 to 0.225 inch. Cracking susceptibility slightly increased when travel speed increased from 5 to 10 inch/minute. Their thermal gradient calculations suggested that the lower travel speed should be used since a narrower temperature gradient is then expected. From the results they suggested that a specimen thickness of 0.312 inch (~8 mm), a current of 190 amps and a weld travel speed of 5 inch/minute (~2 mm/s) should be used as a standard¹¹².

Lippold et al. in an extensive statistical approach for stainless steel and Ni-base evaluated different variables such as arc length, changes of maximum voltage, specimen dimensions, current, weld travel speed, strain range and ram travel speed in Transvarestraint testing. They suggested the current should be kept between 160 and 190 amps and the weld travel speed between 1.7 and 2.5 mm/s for reproducible results¹⁵.

Chapter 4

4 Experimental Procedures

4.1 Materials and Heat Treatments

Four different precipitation hardened Ni-Fe and Ni-based superalloys have been investigated in the present thesis work; Alloy 718 (Ni-Fe-based), Allvac[®] 718Plus[™], Waspaloy and Haynes[®] 282[®]. The materials have been investigated in the mill annealed condition as well as in various heat treatment conditions to evaluate the weldability and in particular the effect on grain size and secondary phase constituents.

Heat treatments were carried out in a vacuum furnace at a heating rate of 0.3 °C/s to specific soak temperatures and dwell times with enforced argon gas cooling employed down to 500 °C and at a cooling rate > 0.3 °C/min.

4.1.1 Alloy 718

The chemical compositions, grain sizes, the material forms and test conditions used for all Alloy 718 weldability tests are shown in table 5 and 6, respectively.

Table 5. Chemical compositions in wt. % of all Alloy 718 material used.

Element	Paper 1	Paper 2	Paper 6 and 9
Ni	Bal.	Bal.	Bal.
Cr	18.41	18.41	18.36
Fe	17.92	17.92	17.49
Co	-	0.17	0.33
Mo	3.05	3.05	3.15
Al	0.60	0.60	0.56
Ti	0.94	0.94	0.92
Nb	5.0	5.0	5.46
C	0.03	0.03	0.04
P	-	0.010	0.008
B	0.002	0.002	0.001
Cu	-	0.13	0.14
Mn	-	0.11	0.09
S	-	0.0004	0.0003
Si	-	0.08	0.05

Table 6. Grain sizes, material forms and test condition of all Alloy 718 materials used.

Alloy 718	Material form	Grain size, ASTM (μm)	Condition
Paper 1	Sheet		As mill annealed
Paper 2	Sheet	8.5 (18.9)	As mill annealed
Paper 6	Wrought bar	11 (7.9), 9 (15.9), 2 (179.6)	954 °C-15 h, 954 °C-1 h, 982 °C-1 h and 1050 °C-3 h + 954 °C-1 h.
Paper 9	Wrought bar	6 (44.9) and 5 (63.5)	954 °C-1 h, 982 °C-1 h, 954 °C-15 h and 1020 °C-1 h.

The heat treatments were carried out for the following reasons:

1. To produce large grains (1050 °C-3 h + 954 °C-1 h and 1020 °C-1h).
2. To produce large amount of δ -phase (954 °C-15 h).
3. The upper and lower recommended standard heat treatment temperature which produces different amounts of δ -phase (954 °C-1 h and 982 °C-1 h).

4.1.2 ATI Allvac[®] 718Plus[™]

The heat treatments of wrought Allvac[®] 718Plus[™] were carried out using the same rationale and heat treatments as for Alloy 718. Standard solution heat treatments at 954 °C-0.5 h were repeatedly used (totally 3 x 0.5 h) for the purpose of stress relief of the forged material at machining and prior EB welding (**paper V**). The chemical compositions, grain sizes, material forms and test conditions of all Allvac[®] 718Plus[™] materials used at weldability testing are shown in table 7 and 8.

Table 7. Chemical compositions in wt. % of all Allvac® 718Plus™ materials used.

Element	Paper 1	Paper 2	Paper 4	Paper 5	Paper 7	Paper 9
Ni	Bal.	Bal.	Bal.	Bal.	Bal.	Bal.
Cr	17.86	18.0	18.0	17.85	17.79	18.0
Fe	9.59	9.6	10.0	9.54	9.53	9.35
Co	8.97	8.9	9.0	9.04	8.99	9.17
Mo	2.70	2.6	2.8	2.67	2.69	2.69
Al	1.49	1.52	1.45	1.43	1.46	1.46
Ti	0.76	0.74	0.7	0.75	0.75	0.75
Nb	5.49	5.47	5.45	5.51	5.47	5.50
C	0.024	0.02	0.025	0.018	0.021	0.02
P	-	0.010	0.014	0.010	0.008	0.005
B	0.004	0.005	0.006	0.004	0.005	0.005
Cu	-	-	-	-	0.01	0.01
Mn	-	0.12	-	0.04	0.05	0.03
S	-	0.0003	-	-	0.0003	0.0003
Si	-	0.08	-	0.04	0.06	0.05
W	0.99	1.0	1.0	1.01	1.02	1.03
V	-	-	-	0.02	0.03	0.02

Table 8. Grain sizes and material forms of all Allvac® 718Plus™ materials used.

Allvac® 718Plus™	Material form	Grain size, ASTM (µm)	Condition
Paper 1	Sheet		As mill annealed
Paper 2	Sheet	10.3 (9.4)	As mill annealed
Paper 4	Cast		As cast, 1125 °C-5 h, 1125 °C-5 h + 1200 °C-5 h and 1200 °C-5 h.
Paper 5	Forging	8 (22.5) and 5 (63.5)	954 °C-1.5 h
Paper 7	Wrought bar	7 (31.8), 6 (44.9) and 3 (127)	954 °C-15 h, 954 °C-1 h, 982 °C-1 h and 1050 °C-3 h + 954 °C-1 h.
Paper 9	Wrought bar	6 (44.9), 5 (63.5), and 3 (127)	954 °C-1 h, 982 °C-1 h, 954 °C-15 h and 1020 °C-1 h.

The homogenization heat treatments in the cast material (**paper IV**) were performed at two different temperatures with the following purpose:

1. Homogenization heat treatment below γ -Laves eutectic temperature to see the effect on homogenization and repair weldability (1125 °C-5 h).

2. Homogenization heat treatment above γ -Laves eutectic temperature to see the effect on homogenization and repair weldability (1200 °C-5 h).
3. A combined homogenization heat treatment which starts below followed by a second step above the eutectic temperature (1125 °C-5 h + 1200 °C-5 h).

4.1.2 Waspaloy

Four different solution heat treatments were used at Gleeble hot ductility testing (paper VIII) as well as for the repair welding investigation (**paper IX**). All four heat treatment (996 °C-4 h, 1010 °C-4 h, 1040 °C-4 h and 1080 °C-4 h) are covered within the AMS specifications where the two high temperature treatments produce larger grain size^{113, 114}. The chemical composition together with grain sizes, material forms and test conditions are shown in table 9 and 10.

Table 9. Chemical composition in wt. % of all Waspaloy materials used.

Element	Paper 2	Paper 8	Paper 9
Ni	Bal.	Bal.	Bal.
Cr	19.13	19.21	19.21
Fe	1.13	1.02	1.02
Co	13.34	13.26	13.26
Mo	4.22	4.04	4.04
Al	1.36	1.32	1.32
Ti	3.03	3.08	3.08
C	0.08	0.033	0.033
P	0.004	0.002	0.002
B	0.006	0.0048	0.0048
Cu	0.02	0.01	0.01
Mn	0.02	0.02	0.02
S	0.002	0.0004	0.0004
Si	0.09	0.06	0.06
Zr	-	0.065	-

Table 10. Grain sizes, material forms and test conditions used for Waspaloy.

Waspaloy	Material form	Grain size, ASTM (μm)	Condition
Paper 2	Sheet	5.7 (44.9)	As mill annealed
Paper 8	Wrought bar	6 (44.9), 5 (63.5), 4 (89.8)	996 °C-4 h, 1010 °C-4 h, 1040 °C-4 h and 1080 °C-4 h.
Paper 9	Wrought bar	6 (44.9), 3 (127) and 2 (179.6)	996 °C-4 h, 1010 °C-4 h, 1040 °C-4 h and 1080 °C-4 h.

4.1.2 Haynes® 282®

The chemical composition, grain sizes, material forms and test conditions used at Gleeble hot ductility testing (**paper III**) are shown in table 11 and 12.

Table 11. Chemical composition in wt % of Haynes® 282®.

Haynes 282	Ni	Cr	Fe	Co	Mo	Al	Ti	C	P	B	Mn	S
Paper 3	Bal.	19.63	0.35	10.35	8.56	1.41	2.21	0.068	0.002	0.004	0.08	0.002

Table 12. Grain size, material form and test condition of Haynes® 282® at Gleeble hot ductility testing.

Haynes 282	Material form	Grain size, ASTM (μm)	Condition
Paper 3	Sheet	5 (63.5) and 1 (254)	As mill annealed, 1121 °C-30 min and 1135 °C-2 h.

4.2 Metallographic Procedures

Metallographic preparations have been carried out through careful cutting using coolant to minimize heat generation. Mounting in conductive Bakelite was performed using Buehler mounting press at pressure of 280 Bar and at a temperature of 180 °C for 8 min followed by water cooling for 4 min. The samples were then grinded using 80, 120, 220, 600, 800 and 1000 grit/inch papers for 90 s at each step together with water cooling. After careful cleaning in water, soap and ethanol polishing was performed on Dur-cloth together with 9 μm and 3 μm size Diamond particles and lubrication media for 180 s at each step. Finally, the etching procedures mainly consisted of two different swabbing techniques; two concentrations of Kalling's etching solution (60 ml Ethanol + 40 ml of HCL or 100 ml Ethanol + 40 ml of HCL) or electrolytically using oxalic acid at 2-5 V for 3-10 s.

At macro etching of cast Allvac® 718Plus™ (**paper IV**) two different solutions were used; Ferric Chloride solution (to bring out grain structure) and Canadian solution (to bring out melt-related defect, mainly segregation). The precise solutions and procedures are as follows:

1. 6 min soak in Ferric Chloride; 90% HCL (32% concentration), 10% HNO₃ (67% concentration), 1 Lb/gal FeCl₃ powder, heated to 45 - 55°C.
2. 6 min soak in Canadian Etch; 2 parts H₂SO₄ (93% concentration), 2 parts HF (49% concentration), 1 part HNO₃ (67% concentration), 8 parts H₂O, heated to 45 - 55°C.

4.3 Microscopy

Examination of the microstructure at first carried out using light optical microscopy (LOM) and followed by scanning electron microscopy (SEM). At LOM a digital imaging software (NIS-Elements D) was used for the evaluation of e.g. grain sizes. In addition to the benefits of high resolution in the SEM standard mode backscattered electron (BSE)

and energy dispersive X-ray (EDX) spectroscopy analyses were used out to identify elemental composition and phases.

4.4 Differential Scanning Calorimetry

Since hot cracking is highly dependent on the solidification range it was decided to determine phase transformations during the heating and cooling sequences (>1100°C) using differential scanning calorimetry (DSC). A constant heating and cooling rate was used while recording the heat flow between reference and sample crucibles during the thermal cycles to interpret phase transformations. A phase transformation will appear as upward (exothermic) or downward (endothermic) peak in the DSC versus temperature curves. The samples were water-jet machined into cylindrical discs of 5 mm diameter and grinded until a weight of approximately 50 mg was achieved. Two different heating and cooling rates were used; 5 °C/min and 20 °C/min with a 20 min isothermal dwell at the soak temperature of 1400 °C between the thermal cycles. In all cases a flow of Ar gas (10 ml/min) as inert protection was used.

4.5 Hardness Testing

Hardness tests were carried out using the Vickers (HV) method. Both micro HV at 1 kilogram force (kgf) and macro HV at 10 kgf were used. Hardness measurements using micro HV were carried out on etched surfaces whereas macro HV were made on the as polished surfaces. An average of five indents was recorded as an average.

4.6 Welding

4.6.1 EB Welding

Electron beam welding (EBW) (**paper V**) was performed in a 30 kW low voltage (60 kV) Sciaky EB welding machine. Circular oscillation at a frequency of 1 kHz was used throughout the complete study. Also, a surface focal point was employed at full penetration EBW. For cosmetic weld passes an above the surface focal point and 10 % heat input relative the nominal was used.

The optimum heat input for each thickness (6, 12, and 20 mm), here called nominal, was determined by trial and error and established after the evaluation of several metallographic cross-sections of EB welds. Important evaluating factors were complete fusion and a minimum weld bead thickness of 2 mm.

Heat input was varied either by separately changing the welding speed, the accelerating Voltage or the current. These changes were adjusted so that the heat input at start of welding was 10 % below nominal and 10 % above nominal at stop position. This was carried out by a linear increase over a distance of 300 mm for each specific parameter previously mentioned.

4.6.2 Repair Welding

At repair welding (**paper IV and IX**), GTAW welding was used together with 1.6 mm diameter filler metal of respective alloy. The specimens were machined after the heat treatment (vacuum heat treatment) and cleaned thoroughly in alkali solution prior to the weld repair to minimize contamination. The actual repair weldings were performed manually by experienced welders at VAC. Ar gas protection was fed through the nozzle surrounding the torch as well as through external units to prevent oxidation.

4.7 Vareststraint and Transvareststraint Testing

Vareststraint and Transvareststraint testing were performed to study the HAZ liquation and solidification cracking (**paper I and II**). Here, cracking is produced by the augmented strain as schematically shown in figure 9.

Sheet coupons were water-jet machined from the superalloy sheets. The longitudinal direction of the test coupons were the same as the rolling direction, even though no texture could be detected. Transvareststraint testing was used to evaluate the susceptibility towards solidification cracking whereas Vareststraint testing mainly was used for determining cracking susceptibility to HAZ liquation cracks.

The welding parameters used in the experiment reported in paper I and II were the same except that the Allvac[®] 718Plus[™] material in paper I was slightly thinner (2.9 mm compared with 3.2 mm) which was compensated for by using a lower welding current (70 A) to produce the same weld characteristics. The nominal parameters were set to a current of 85 A using DCEN and a 2.4 mm diameter La₂O₃ electrode at a welding speed of 2 mm/s. Different Vareststraint mandrel radii were used to produce varying amount of augmented strain. A ram speed of 16 mm/s was used in both studies. A ram speed of 43 mm/s was also tested in paper I.

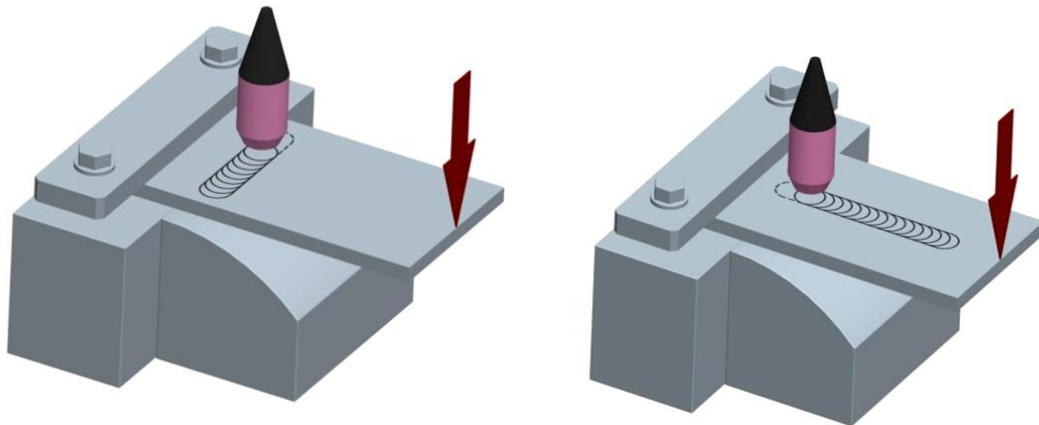


Figure 9. Schematic view of the Transvareststraint and Vareststraint test, respectively¹⁰³.

After testing, the total crack length (TCL) was measured as a way of evaluating the crack susceptibility. The evaluation was done using both stereo microscope (**paper I**) and on fluorescent penetrant inspection images (**paper II**). Before and after every Vareststraint test, side view photos were captured to study the kinking behaviour of the plates since no support plates were possible to use in order to reduce this effect.

4.8 Gleeble Testing

The Gleeble specimens were manufactured from bar stock (Alloy 718, Allvac[®] 718Plus[™] and Waspaloy) by electric discharge machining followed by vacuum heat treatment at specific schedules and finally machined to test dimension by turning. The Haynes[®] 282[®] material was water-jet machined from 3.2 mm thick sheet followed by heat treatments. The actual testing was carried out in a 1500D Gleeble machine using the parameters shown in table 13.

Table 13. Gleeble hot ductility testing parameters of Alloy 718, Allvac[®] 718Plus[™], Waspaloy and Haynes[®] 282[®] (papers III and VI to VIII).

Gleeble parameters	
Heating rate	111 °C/s
Cooling rate	50 °C/s
Peak temperature	1195 (Alloy 718), 1200 (Allvac[®] 718Plus[™]), 1240 (Waspaloy) and 1250 (Haynes[®] 282[®]) °C
Stroke rate	55 mm/s
Holding time at peak temperature	0.03 s
Holding time at test temperature	0.03 s
Thermocouple and diameter	Chromel-alumel and 0.254 mm

Chapter 5

5 Summary of Results in Appended Papers

The work presented in this thesis comprises the results reported in the nine appended papers (**papers I-IX**) and is briefly summarized in the following sections.

5.1 Paper I and II

The sheet materials in paper I and II have been tested in the as-received or mill-annealed conditions.

Comparisons in terms of TCL vs. augmented strain in Transvarestraint testing as well as TCL vs. calculated strain in Varestraint were made. Both testing methods encountered problem due to kinking, that is, the material did not perfectly adhere to the mandrel die surface as intended. The Allvac[®] 718Plus[™] material did reveal more kinking compared to Alloy 718 during the Transvarestraint testing even though it cracked less, figure 10.

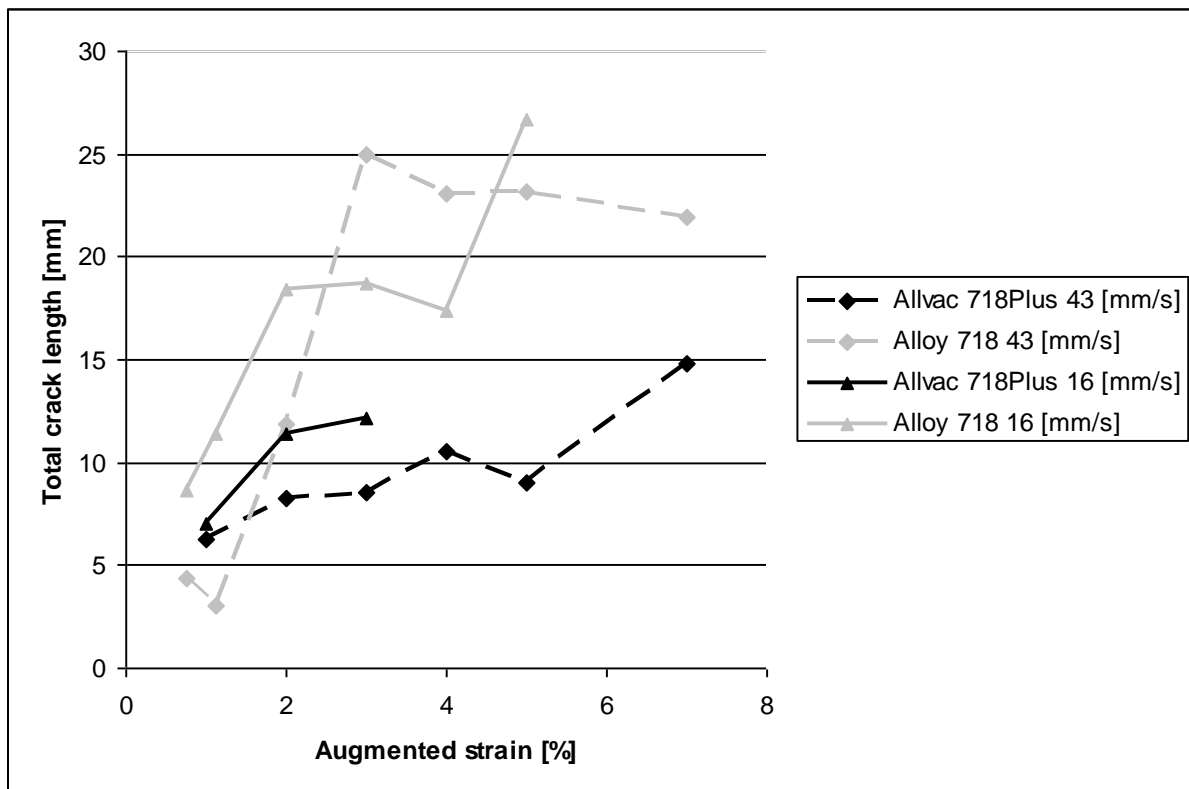


Figure 10. Transvarestraint testing. Total crack length [mm] as a function of augmented strain [%] for Allvac[®] 718Plus[™] and Alloy 718 at 16 mm/s and 43 mm/s strain rate.

Despite the large scatter (especially for Allvac[®] 718Plus[™]), Waspaloy undoubtedly is the most crack resistant alloy in comparison with the other two as is indicated in figure 11.

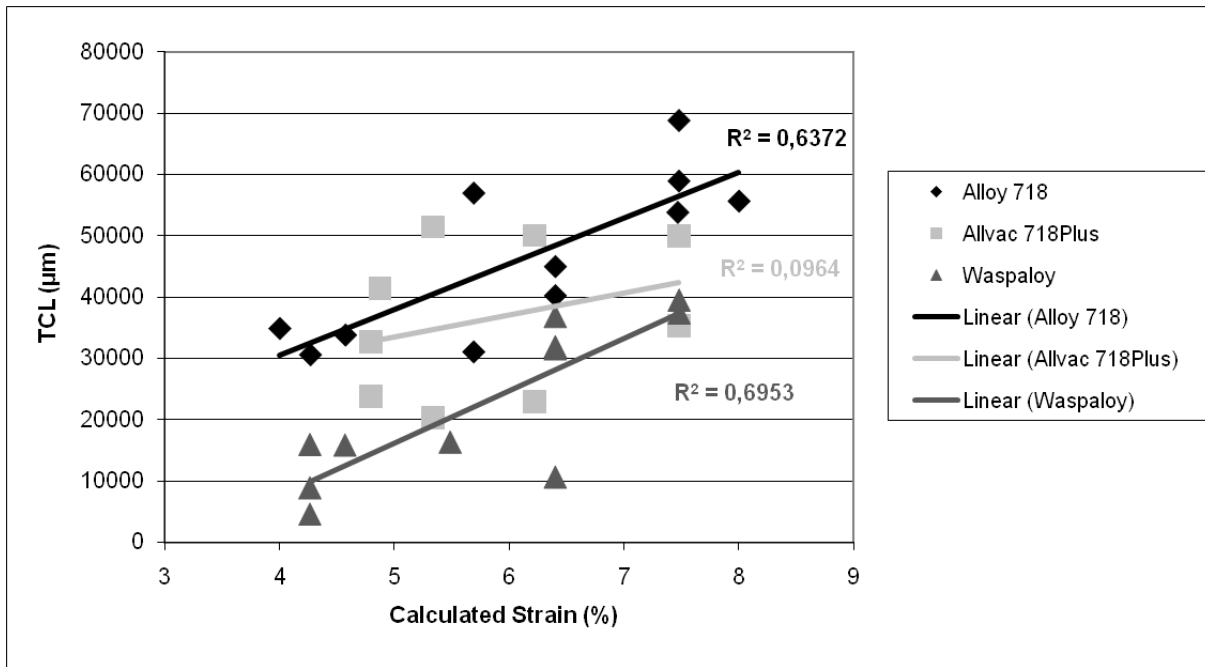


Figure 11. Varestraint testing. TCL [µm] against calculated strain [%] together with regression values for each trend-line.

The better cracking resistance can simply be explained by the summary of the DSC experiment in table 14 which reveals a much narrower solidification range for Waspaloy in comparison with both that of Allvac[®] 718Plus[™] and of Alloy 718, which are similar. There is one eutectic phase reaction during solidification of Waspaloy and two eutectic ones in Allvac[®] 718Plus[™] and in Alloy 718.

The solidification sequences of Allvac[®] 718Plus[™] and Alloy 718 starts with the solidification of the γ phase followed by the γ -MC reaction (1260 – 1275°C) and ends by the γ -Laves eutectic reaction (~1160°C). Waspaloy begins to solidify at a slightly higher temperature and ends by a γ -MC reaction (~1245°C).

Table 14. Results of DSC Experiments.

Alloy/Phys. prop.	T _L °C	T _S °C	y/MC eut. °C	y/Laves eut. °C	Melt. range/Sol. Int.
Alloy 718					
5K heating	1347	-	1277	1169	178
5K cooling	1343	-	1261	-	82
20K heating	1351	-	1272	-	79
20K cooling	1334	-	1226	1158	177
Allvac 718Plus					
5K heating	1370	-	1266	1143	227
5K cooling	1351	-	-	-	-
20K heating	1350	-	1275	-	75
20K cooling	1340	-	1275	1158	182
Waspaloy					
5K heating	1370	1316	-	-	55
5K cooling	1365	1316	-	-	50
20K heating	1375	1310	-	-	65
20K cooling	1358	-	1245	-	113

Conclusions from these two papers are:

1. Allvac[®] 718Plus[™] alloy exhibits less solidification cracking than standard Alloy 718.
2. The solidification cracking is clearly related to the eutectic phase constituents such as Laves phase and MC carbides, and where Alloy 718 seems to exhibit a larger amount of these constituents.
3. Total amount of hot cracking of Waspaloy is much less than in Alloy 718 and in Allvac[®] 718Plus[™].
4. The lower susceptibility to hot cracking of the Waspaloy in comparison with Alloy 718 and with Allvac[®] 718Plus[™] can be associated with the presence of the Laves eutectic for the latter two and a corresponding larger solidification range.

5.2 Paper III

Gleeble hot ductility testing was carried out on Haynes[®] 282[®] sheet material in three different conditions to investigate the effect on different solution heat treatments and grain size in particular. The hot ductility response to the different solution heat treatments is shown in figure 12. It was concluded that increased grain size (ASTM 1) achieved through heat treatment at 1135 °C for 2 hours reduces the hot ductility in comparison with the as mill-annealed and 1121 °C-30 min conditions. The onset of liquation was attributed to carbide liquation but no characterization was made to confirm this observation.

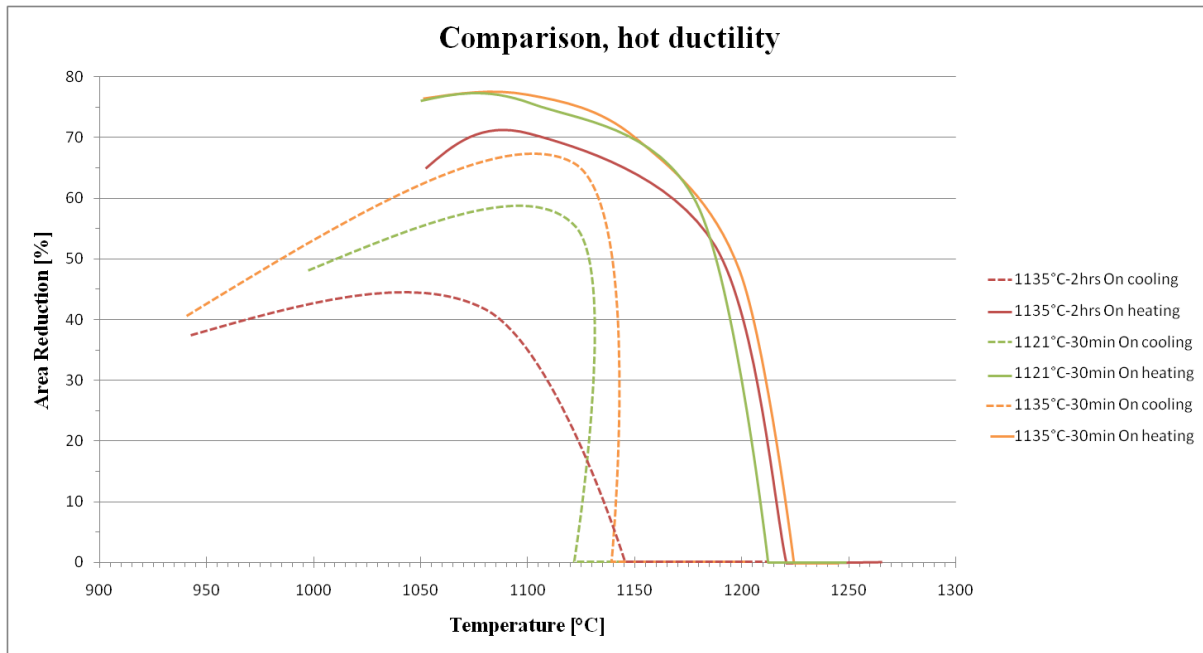


Figure 12. Hot ductility of Haynes[®] 282[®] at different solution heat treatments.

The Gleeble hot ductility parameters together with weldability parameters are shown in table 15.

Table 15. Gleeble hot ductility and weldability parameters of Haynes[®] 282[®].

	1121 °C-30 min	Mill Annealed	1135 °C-2 h
Nil Strength Temperature, [°C]	1260	1260	1260
Nil Ductility Temperature, [°C]	1210	1225	1220
Ductility Recovery Temperature, [°C]	1120	1140	1140
Brittle Temperature Range, [°C]	140	120	120
Ductility Recovery Rate, [%]	74	86	56
Ratio of Ductility Recovery, [%]	32	44	18

The following conclusions were made from the Gleeble hot ductility study:

1. Alloy Haynes[®] 282[®] exhibits good hot ductility with a narrow brittle temperature range of 110-125°C for the specific conditions tested which advocates a good weldability.
2. The hot ductility of the as-received material (bright annealed in a continuous heat treating furnace at 1121-1150 °C for about 30min and quenched) is equivalent to that of the low temperature (1121 °C) short time (30min) re-solutioned material.
3. Large grain size (ASTM 1) obtained by grain growth at the high temperature (1135 °C) long time (2 h) re-solution heat treatment lowers the hot ductility

compared with the as-received fine grain condition (ASTM 5) by 17% and 7% in terms of ductility recovery rate and ratio of ductility recovery, respectively.

4. A Vickers hardness increase of 103 units during the cooling down heat treatment cycle from the 1121 °C solution temperature indicates a risk for strain age cracking at post-weld heat treatments.

5.3 Paper IV

Repair welding at different stages of homogenization was performed on stair case (three different sections) plates of cast Allvac[®] 718Plus[™] material. The homogenization heat treatments clearly showed that the amount of Laves phase decreases for dwell times greater than 5 hours as seen in figure 13 but at shorter dwell times at lower temperatures, the amount of Laves phase actually increased as shown in figure 14.

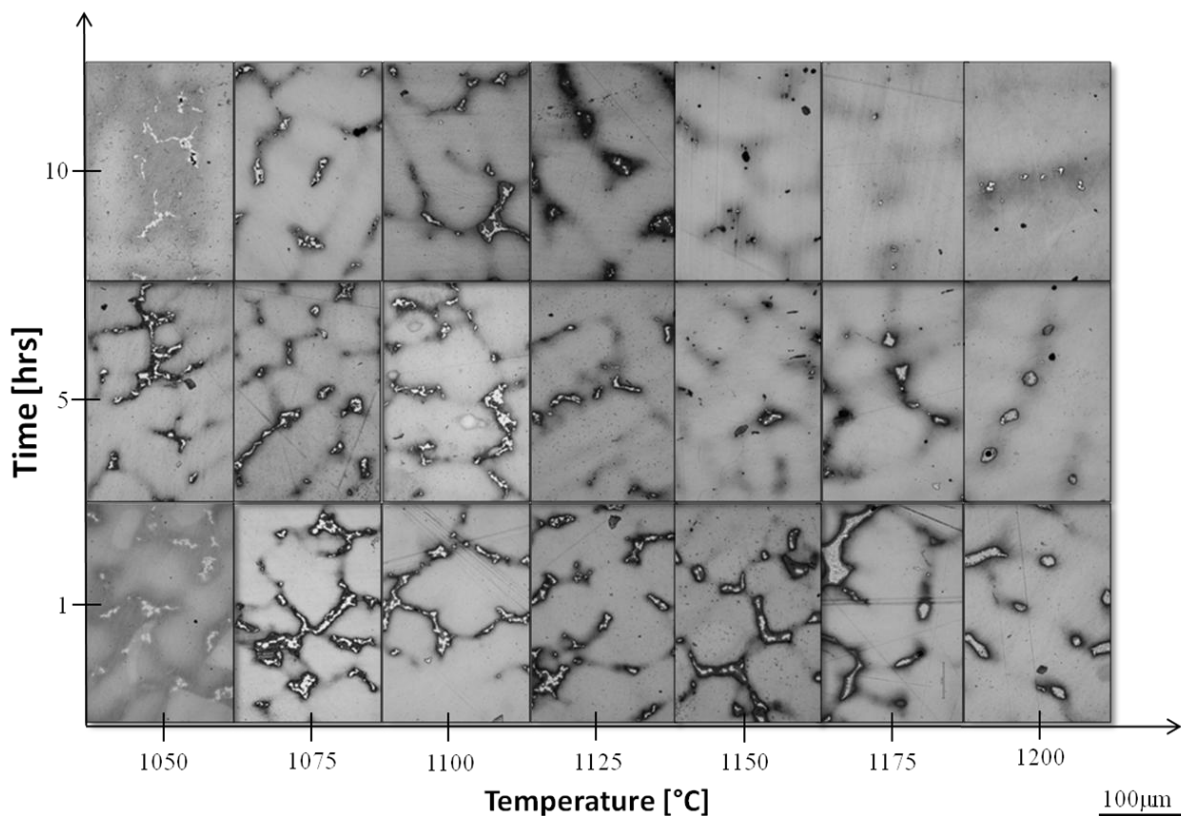


Figure 13. Microstructure response of the homogenization heat treatments from 1050 °C to 1200 °C in steps of 25 °C and at 1 h, 5 h and 10 h, respectively.

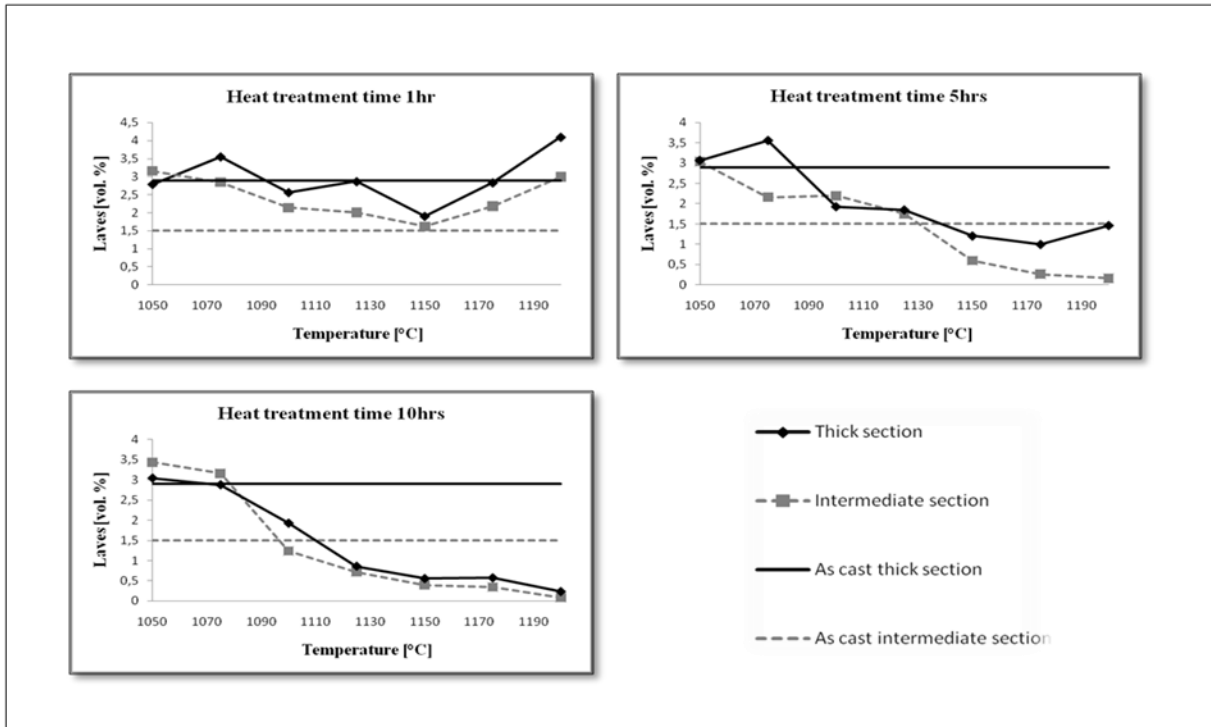


Figure 14. The amount of Laves phase versus temperature for the three different heat treatment times for the thick and intermediate sections in comparison. The upper horizontal lines represent the measured amounts of Laves phase for the thick section in the as-cast condition and the lower line for the as cast condition in the intermediate section.

Surprisingly, at the repair welding trials it was seen that the most homogenized state revealed most cracking whereas the low temperature homogenization heat treatment was found to be best suitable, figure 15.

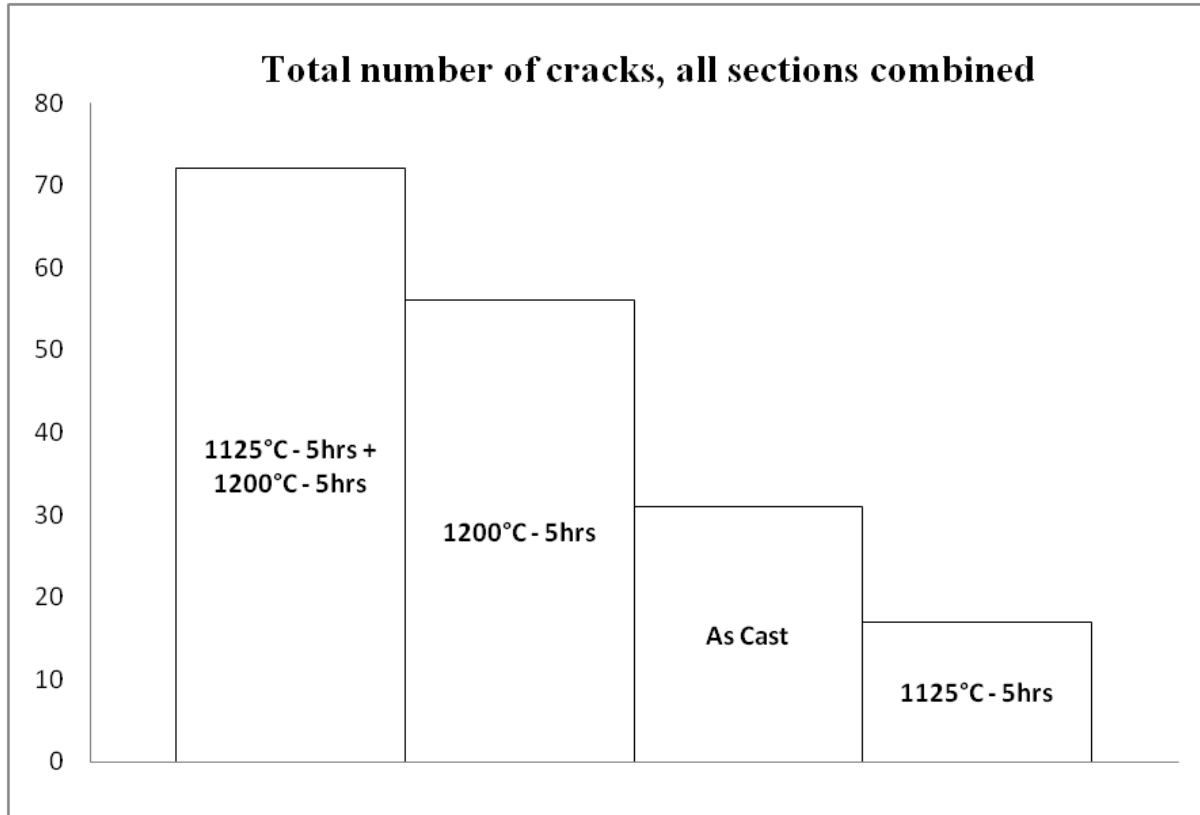


Figure 15. Total number of cracks in weld cross sections for different homogenization heat treatment conditions.

Based on the homogenization studies together with the repair welding trials the following was concluded:

1. At the lowest homogenization temperatures (1050 °C and 1075 °C) no dissolution of the Laves phase occurred even after 10hrs dwell time.
2. The amount of Laves phase increased at the initial stages of homogenization at the lowest temperatures and especially for the finer structure of the intermediate section.
3. Heat treatments at 1175 °C and above will result in melting of the Laves eutectics and faster dissolution of the Laves phase.
4. No long-range homogenization across dendrites was observed.
5. Macro Vickers hardness measurements reveal a rapid increase in hardness upon first stages of homogenization but no further increase with time and temperature was noted.

6. Surprisingly the most homogenized material 1125 °C-5 h + 1200 °C-5 h was the most susceptible condition to weld cracking and considerably more susceptible than the material in the as-cast condition.

5.4 Paper V

EBW of Allvac® 718Plus™ forged rings was carried out and reported in paper V. Three different thicknesses (6, 12 and 20 mm), two grain sizes (ASTM 5 and 8) and different welding parameters were investigated. No open cracks, regardless of thickness, grain size or welding parameters, were found. Metallographic analyses, however, revealed that a significant number of healed cracks were present, as illustrated in figure 16.

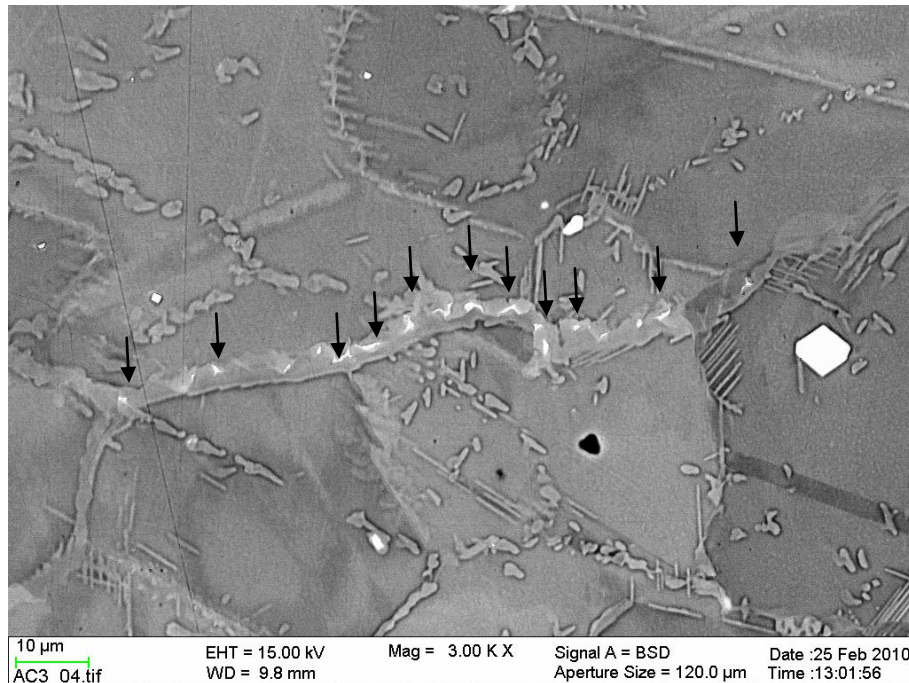


Figure 16. SEM-BSE micrograph reveals a healed crack including a phase constituent of script morphology (indicated by the arrows).

The healed cracks contain constituents with a script morphology which is typical for the Laves phase indicating that a Laves eutectic reaction has taken place during the solidification of a liquid phase which back filled the cracks. Since δ phase contains a large amount of Nb and due to the fact that δ phase was found adjacent to these cracks it was suggested that the δ phase played an important role in the healing of cracks in the HAZ through constitutional liquation. This phase reaction may be explained by the pseudo binary phase diagram as shown in figure 17 below.

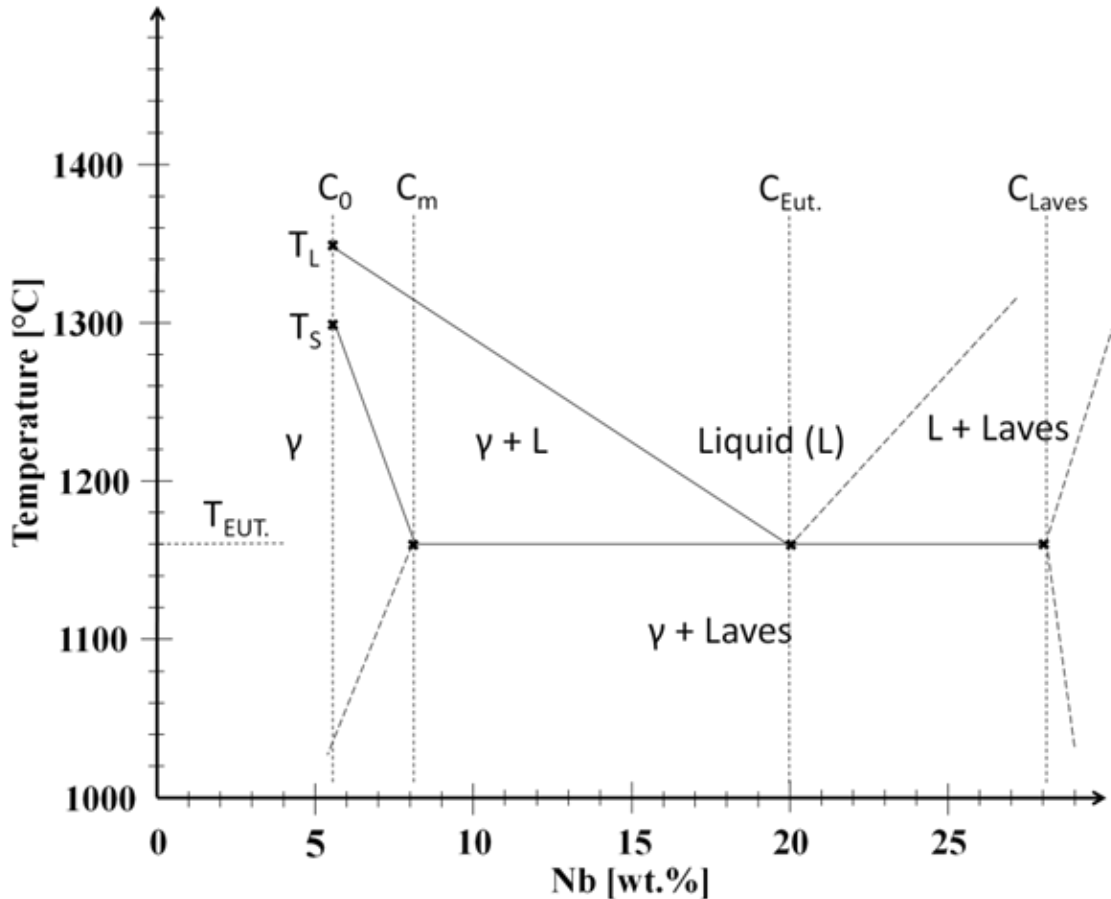


Figure 17. Pseudo-binary phase diagram for Allvac® 718Plus™.

Constitutional liquation can only occur if a eutectic reaction is possible from a compositional point of view. With reference to the pseudo-binary diagram in figure 17 this amounts to the fact that a Laves eutectic reaction can only take place if there is a local concentration (above the nominal (C_0) composition) of Nb and which is higher than maximum solubility (C_m) of Nb at roughly 8 wt % at the eutectic temperature T_{EUT} . Since the δ phase contains more than 8 wt % Nb it is quite possible that the presence of this phase may supply enough Nb locally provided the heating is fast enough to avoid dissolution and excessive downhill diffusion. Such fast heating is quite possible in the EB-welding process.

The conclusions from paper V were:

1. No “open” cracks were found.
2. Backfilled cracks were found at the top, root and in the heat affected zone.
3. δ -phase undergoes constitutional liquation rather than dissolving through the solid state diffusion in the heat affected zone.

4. δ -phase assists healing of cracks through liquation, in the heat affected zone.

5.5 Paper VI-VIII

An extensive Gleeble hot ductility investigation was carried out on Alloy 718, Allvac[®] 718Plus[™] and Waspaloy to study the effect of four different solution heat treatments and reported in paper VI-VIII. The ductility as the reduction of area (RA) was determined at different temperatures and thermal cycles to establish the hot ductility signatures of these three alloys are shown in figures 18 through 21.

Alloy 718 and Allvac[®] 718Plus[™] was heat treated at 954 °C-1 h, 982 °C-1 h (standard heat treatments), 954 °C-15 h (to produce large amount of δ phase) and at 1050 °C-3 h + 954 °C-1 h (to produce large grain size).

It was found that constitutional liquation of NbC was assisted by δ phase to deteriorate the ductility. However, parameters associated with weldability (BTR, DRR and RDR) advocated a improved weldability for the condition with a large amount of δ phase whereas the coarse grain size condition was seen to deteriorate the ductility situation for Alloy 718 as indicated in table 16 and 17.

The δ phase was considered to be beneficial, if present in sufficient amount, by a grain boundary pinning effect. With limited grain growth at the very high temperatures the large grain boundary area of the fine grain material could be maintained and thus reduce the effect of the trace elements at the grain boundaries.

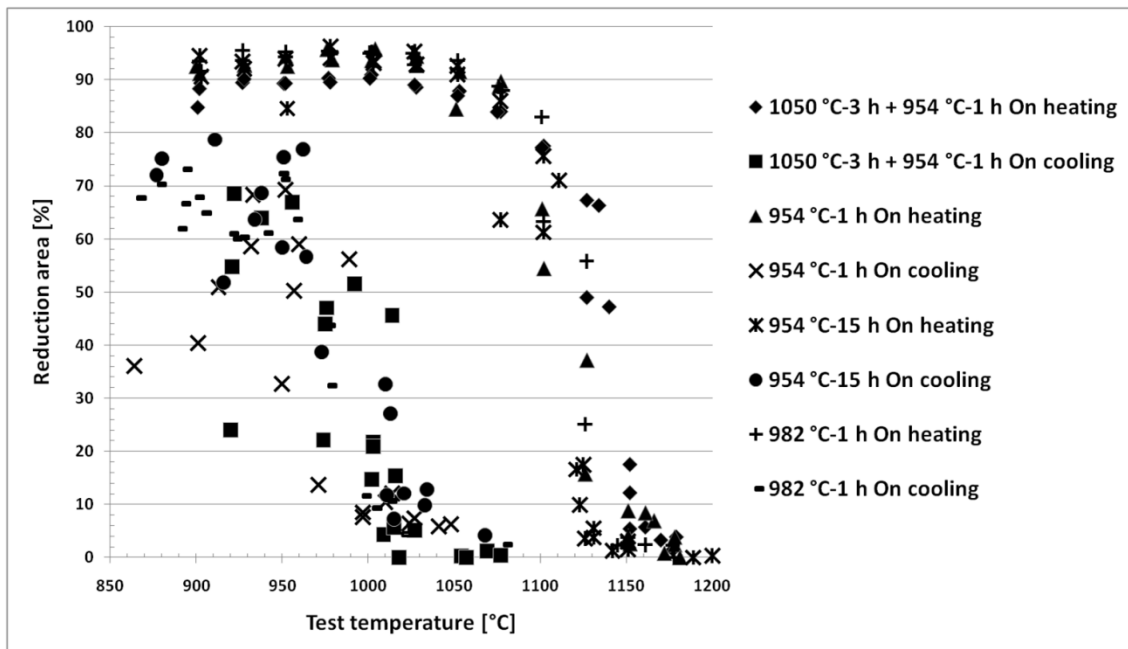


Figure 18. The hot ductility of Alloy 718 in the four different heat treated conditions versus temperature in the on-heating and on-cooling test cycles.

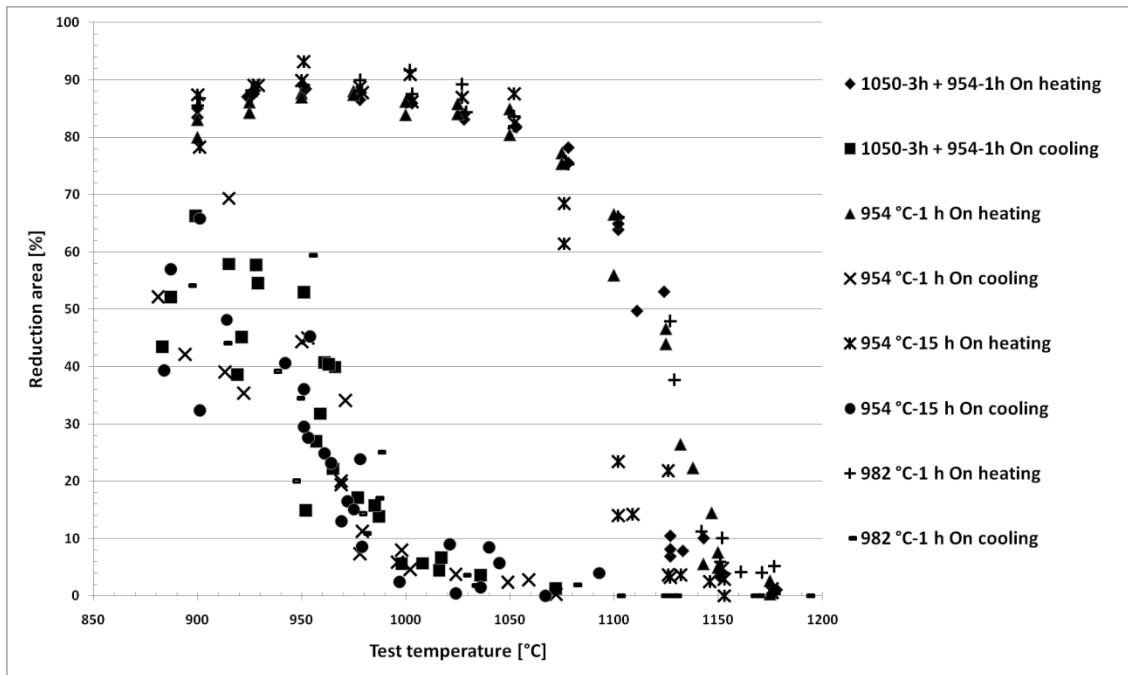


Figure 19. Reduction of area versus temperature for different solution treatments of Allvac® 718Plus™.

Table 16 Estimated Gleeble/weldability parameters of Alloy 718.

Treatments	NDT	BTR	DRR	RDR	Score	Ranking
954 °C-1 h	2	2	4	3	11	3
982 °C-1 h	3	3	2	2	10	2
954 °C-15 h	4	1	1	1	7	1
1050 °C-3 h + 954 °C-1 h	1	4	3	4	12	4

Table 17 Estimated Gleeble/weldability parameters of Allvac® 718Plus™.

Treatments	NDT	BTR	DRR	RDR	Score	Ranking
954 °C-1 h	4	4	1	3	12	4
982 °C-1 h	1	3	4	2	10	3
954 °C-15 h	2	1	3	1	7	1
1050 °C-3 h + 954 °C-1 h	3	2	2	2	9	2

Waspaloy on the other hand, was heat treated at 996 °C-4 h, 1010 °C-4 h, 1040 °C-4 h and 1080 °C-4 h were the last two treatments are above the $M_{23}C_6$ and γ' solvus temperatures and consequently they allow for grain growth. In figure 20 the on-heating ductility signatures are shown and in figure 21 the on-cooling ductility.

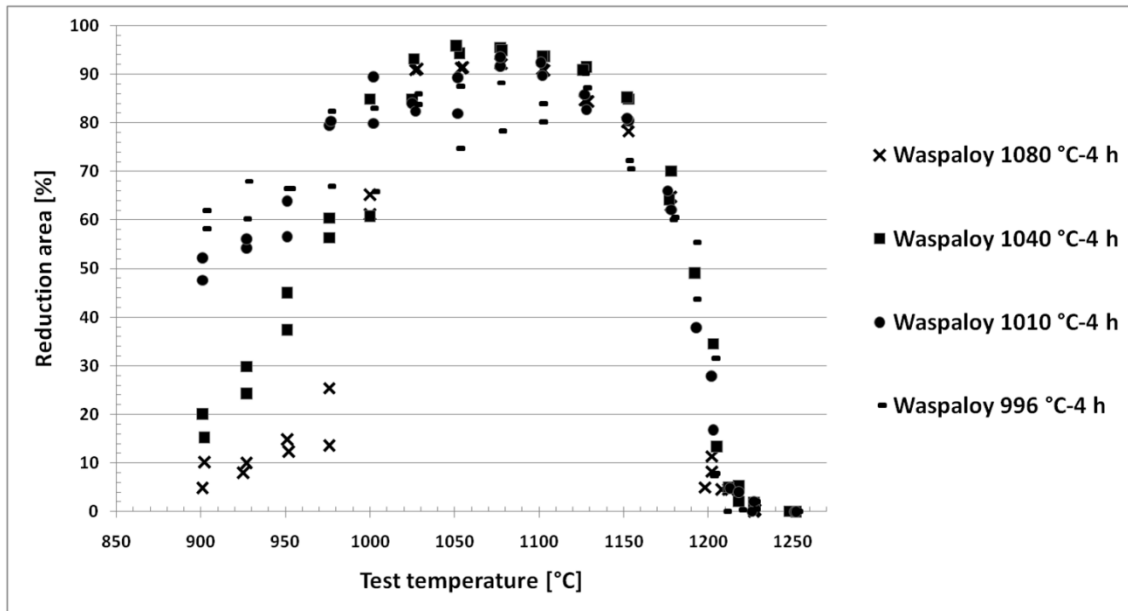


Figure 20. On-heating hot ductility, RA versus temperature in the four different solution heat treatment conditions.

The on-heating ductility signature below 1050 °C was attributed to the particle size and distribution of the γ' and $M_{23}C_6$ phases which differed significantly. The complete dissolution of these precipitates was found to explain the predominantly ductile fracture behavior at 1100 °C. The grain boundary liquation mechanism in Waspaloy was associated with the presence of B at liquated grain boundaries as confirmed by SEM-EDS analyses.

The on-cooling ductility graph in figure 21 indicates that the 1080 °C-4 h treatment is the only one which renders a ductility recovery upon cooling and is consequently advocated to be most suitable heat treatment from a weldability perspective.

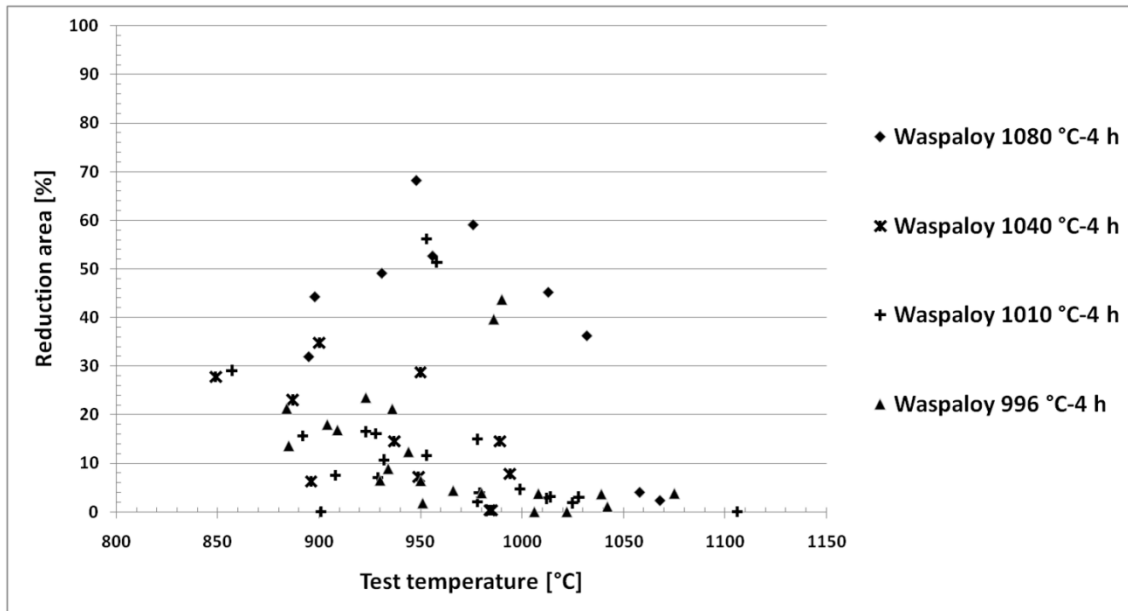


Figure 21. Waspaloy on-cooling hot ductility, RA versus test temperature in the four different solution heat treatment conditions.

The conclusions for Alloy 718 and Allvac[®] 718Plus[™] can be summarized as follows:

1. Based on Gleeble testing it is indicated that a coarse grain material (ASTM 3) forecasts limited weldability in Alloy 718.
2. The δ phase is believed to be beneficial through a grain boundary pinning effect if present in significant amounts and thus reducing the grain growth and consequently also reducing the concentration (per area unit) of the trace elements at the grain boundaries at very high temperatures.
3. Grain boundary δ phase was found to assist the constitutional liquation of the NbC phase.
4. Significantly different solution heat treatments and with associated substantial variations of the microstructure affected the Gleeble test hot ductility only to a very limited extent.
5. A ranked indicator for weldability is suggested based on established evaluation criteria for Gleeble ductility testing.

The Gleeble hot ductility investigation of Waspaloy gave the following conclusions:

1. The on-heating ductility of Waspaloy is governed by the presence of γ' and $M_{23}C_6$ phases up to ~ 1050 °C where maximum ductility is reached irrespective of pre-solution heat treatment.

2. The ductile to brittle transition starts at ~1100 °C.
3. Indications were found that segregation of B may assist liquation in Waspaloy at temperatures well below the eutectic liquation temperature of the MC phase.
4. The 1080 °C-4 h treatment is the only condition which renders a recovery of the ductility in the on-cooling thermal cycle; RA 60 % at 980 °C.

5.6 Paper IX

At multi pass repair welding of Alloy 718, Allvac[®] 718Plus[™] and Waspaloy it was seen that SAC did occur in addition to hot cracking. Significant hardening took place in the bottom layer of multiple layer welds in Allvac[®] 718Plus[™] and Waspaloy and is thus associated with SAC in this part of the repair weld.

Alloy 718 exhibited the best repair weldability followed by Allvac[®] 718Plus[™] and Waspaloy as measured by the number of cracks both in the HAZ and in the FZ. The coarse grain materials, produced by super-solvus treatments, significantly increased the susceptibility to cracking in the HAZ for all three superalloys which for Waspaloy actually contradict what the Gleeble hot ductility testing results suggest. This contradiction may be associated with the much steeper temperature gradient in a GTAW process compared with gradient in the Gleeble testing and where grain growth is not promoted to the same extent, hence, reducing the degrading grain boundary sweeping act which was believed to take place at Gleeble on-cooling tests.

It was found that a large amount of δ phase in Alloy 718 and Allvac[®] 718Plus[™] is beneficial for repair weldability which supports what was suggested by the Gleeble hot ductility investigation (**Paper VI and VII**). As expected no correlation between the pre-solution heat treatments and FZ cracking could be seen.

Chapter 6

6 Concluding Remarks

6.1 Conclusions

The following conclusions on the weldability of precipitation hardening superalloys can be drawn from the results presented in the papers I-IX:

1. Transvarestraint testing and Varestraint testing are representative testing methods for solidification cracking and HAZ liquation cracking.
2. Gleeble testing results can to some extent be associated with HAZ liquation cracking but with contradicting results with the repair welding of Waspaloy. This emphasizes the general difficulties to compare GTAW with Gleeble hot ductility testing results.
3. Solidification cracking and HAZ liquation cracking is aggravated by the presence of γ -Laves eutectic reaction since it extends the solidification temperature range. Since there is no γ -Laves eutectic reaction in Waspaloy it is less susceptible to HAZ liquation cracking compared with Alloy 718 and Allvac 718Plus.
4. HAZ liquation cracking is associated with constitutional liquation of NbC in Alloy 718 and Allvac[®] 718Plus[™].
5. The δ phase was found to assist constitutional liquation of NbC in Alloy 718 and Allvac[®] 718Plus[™].
6. The δ phase was found to improve the weldability for Alloy 718 and Allvac[®] 718Plus[™] which was attributed to the improved ability to heal cracks and to inhibiting grain growth.
7. Trace elements segregation to grain boundaries was associated with grain boundary liquation in Waspaloy.
8. SAC takes place during repair work on Allvac[®] 718Plus[™] and Waspaloy with Waspaloy as the alloy most vulnerable to cracking followed by Allvac[®] 718Plus[™] and Alloy 718.
9. Large grains enhance HAZ liquation cracking.
10. Homogenization heat treatment above the γ -Laves eutectic temperature deteriorates the weldability of cast Allvac[®] 718Plus[™].
11. Homogenization heat treatment below γ -Laves eutectic temperature improves weldability of Allvac[®] 718Plus[™] in comparison with the as cast material.

6.2 Industrial and Scientific Contribution

The industrial and scientific contributions of the present work can be summarized as follows.

- Different techniques as Vareststraint testing, Gleeble testing and repair welding are necessary for the evaluation of the weldability from a general industrial point of view.
- By combining various techniques it has been possible to evaluate the cracking susceptibility during welding of alloys such as Alloy 718, Allvac[®] 718Plus[™] and Waspaloy
- From a metallurgical scientific point of view it has been possible to show that δ phase contrary to the general belief improves the weldability due to its ability to inhibit grain growth and to assist in the healing of cracks.

Chapter 7

7 Future Work

As may be understood from the work presented in this thesis the “weldability” of a specific superalloy material may be characterized by combining different weldability testing methods in a way which makes a comparison with other similar alloys both meaningful and consistent with “intuitive industrial practice”. However, measuring the susceptibility to cracking from a fundamental metallurgical perspective for later incorporation in the modelling of welding to forecast the limits is still far away.

With this aim it is thus appropriate to strive for a coupled (thermo-mechanical and metallurgy) approach for the future of the weldability testing where criteria like threshold strain and cracking temperature interval together with specific weld parameters can be introduced to the weld modelling. For this purpose an initiative was taken to develop a modified Varestraint testing method (shown in figure 22) where it is possible to perform Varestraint, Transvarestraint and spot-varestraint testing at ram speeds from 15 to 300 mm/s.

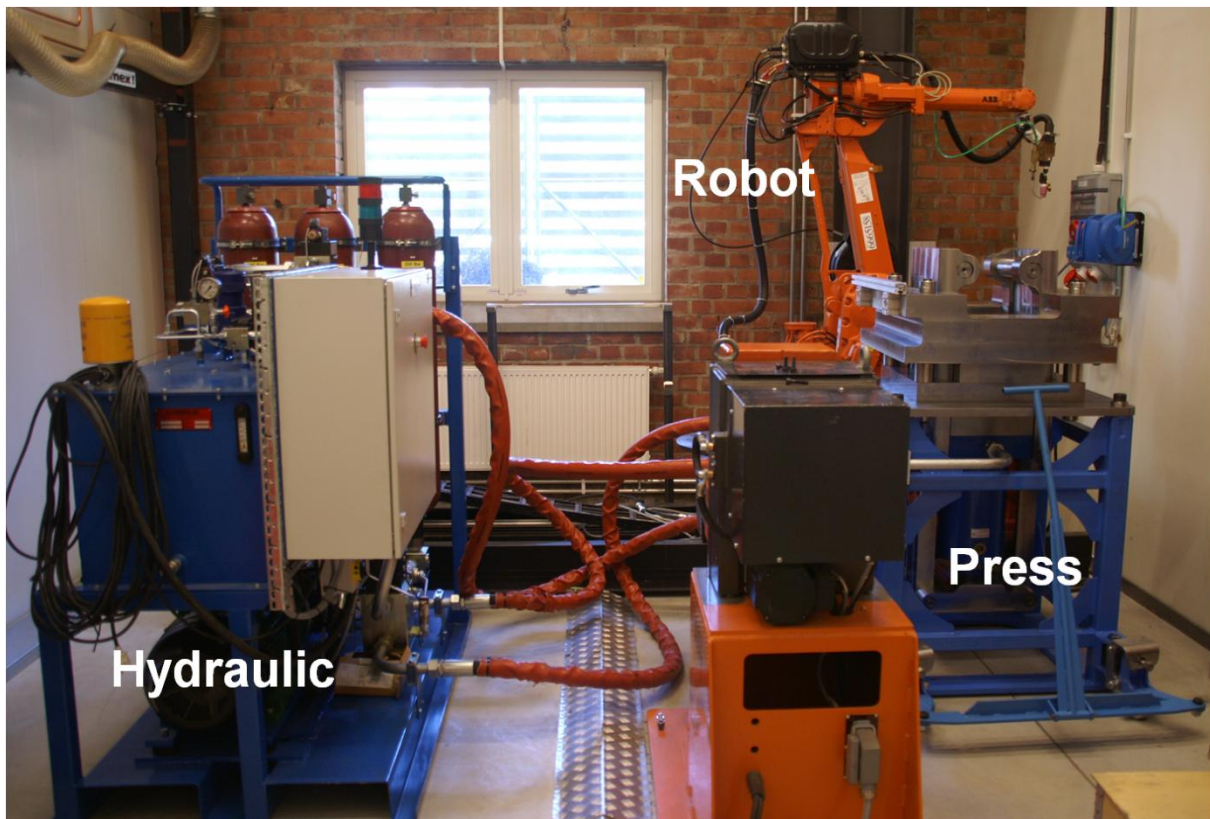


Figure 22. A newly developed weldability testing machine.

The idea is to use the testing machine together with a welding robot and using different welding processes such as GTAW, plasma arc welding and laser welding. The plan is

also to test weld filler metals and multipass welding in addition to traditional testing for bead on plate welding. This will be an approach close to the practical weld situation in industrial practice supplemented with elaborate metallurgical evaluation through a generic methodology.

Acknowledgements

Alma! You have always been there for me during these years showing your love and support even at times of struggle and when I've been far away in my mind. I would never have been able to manage this work without your tremendous support. Thank you, I love you!

I sincerely thank Prof. Göran Sjöberg, my supervisor, colleague and friend. I thank you for your guidance, time and support. You have given me the opportunity and space to grow in different aspects which have been invaluable to me, thank you for trusting in me! I also thank your wife Savoi Alit Sjöberg for supporting you which has been in favour for me.

I've been very privileged to spend these years at the department of Materials Technology at Volvo Aero Corporation. I've had great assets to various equipments day and night seven days a week. I thank all the people working at the Materials Technology department (9651 & 9653) for their support in different aspects. I especially thank Mr. Bengt Pettersson, Mr. Johan Ockborn, Mr. Johan Tholérus, Mr. Frank Skystedt and Mr. Anders Björnson for valuable discussions and co-operation in present research projects as well as others, Mr. Leif Skoog and Mrs. Birgitta Augustsson for fruitful advice regarding metallographic procedures. I thank Dr. Henrik Tersing at the Manufacturing Simulation department for good collaboration and Mr. Anders Sjunnesson at the department of Advanced Engineering for support during the VITAL project. I'm grateful to Mr. Joakim Skoog manager for the Fabrication & Special Processes department who opened the door for me to join the Materials department some years ago.

There are many other people which I've had the pleasure to come across during these years.

At the department of Materials and Manufacturing Technology at Chalmers University of Technology in Gothenburg I thank Prof. Lars Nyborg (head of the department) for his support, not at least financially! I thank my group leader Prof. Uta Klement for her support. I thank my former roommate at Chalmers Lic. Eng. Stefan Olovsjö and Mr. Stefan Cedergren for our interesting discussions and collaboration. At the department of Microscopy and Microanalysis I thank Lic. Eng. Leif Viskari for his help and co-operation in SEM analysis and in reviewing some of my papers. I also thank Prof. Krystina Stiller for helping me by providing time in her SEM instrument.

At the department of Inorganic Chemistry at Göteborg University I thank Dr. Christopher Knee for helping out with thermal analysis.

I had the great pleasure of being acquainted to Mr. Sathiskumar Jothi, Ms. Josefin Larsson (co-author to paper III), Mr. Aurélien Alboussièrre and Mr. Xiangbin Xiao as being their supervisor during their master thesis work. I wish you all good luck!

I would like to express my sincere thanks to my Finnish friends at the department of Engineering Design and Production, Engineering Materials at Aalto University School of

Science and Technology in Helsinki, Finland. In total I've spent about 8 months at your department dealing with Varestraint testing and development work which is planned to be an integral part of future Varestraint testing, work which I unfortunately haven't had time to dig into yet but I know what to do for the years to come. I thank Prof. Hannu Hänninen for great co-operation and financial support, Lic.Sc. (Tech.) Anssi Brederholm for helping out with many things but especially the Varestraint testing. I also thank Mr. Kim Widell for help with heat treatments, Mr. Hessu Vestman (the best welder in Finland) for help with weld fixturing, M.Sc. (Tech.) Miikka Aalto for help with strain gauges, M.Sc. (Tech.) Tapio Saukkonen for help with SEM-analyses, Mr. Janne Peuraniemi for help with the CNC machine, Ms. Laura Tiainen for help in the laboratory and Ms. Johanna Salmela for help with administrative issues.

At the department of Mechanical and Industrial Engineering at the University of Manitoba in Winnipeg, Canada I would like to give my token of gratitude to Prof. Emeritus Mahesh Chaturvedi for giving me the opportunity to come (several times) to your department to perform research. At one time I almost managed to blow up the whole Gleeble machine, but it was fixed by your staff and I was welcomed back to perform another thousands tests or so. Thank you! I thank Dr. O. A. Ojo for all help during my stays, for nice discussions and advice regarding my research both in Winnipeg and by email correspondence afterwards, Dr. Krutika Vishwakarma and Mr. Mike Boskwick for teaching me how to run the Gleeble machine.

I thank Mr. Rich Jeniski at ATI Allvac in Monroe USA for hosting me at the plant a couple of times (I will never forget the Kobe steak in Pittsburgh). I thank Dr. Henry White at Haynes International in Kokomo USA for fruitful discussions and for organizing my two visits to the Kokomo facility. I thank Dr. Mike Santella and Dr. Zhili Feng, respectively, for taking care of me when visiting the Oak Ridge National Laboratory in Knoxville USA. I thank Prof. John Lippold at welding lab of the Ohio State University USA for giving me the opportunity to visit his department (apart from the hot cracking workshop) together with the Edison welding institute. I thank Prof. Lars-Erik Svensson at University West for fruitful discussions regarding welding.

There have been three companies involved in the development of the weldability testing machine apart from Volvo Aero; A TEKNIK AB, MIDROC ELECTRO AB (Division Automation) and PMC CYLINDERS AB (CA-Verken). First of all I thank our research director at Volvo Aero, Dr. Henrik Runnemalm, for giving me this opportunity and for providing the financial resources to fulfill this task. I thank Mr. Kenneth Nylén and Mr. Bengt-Arne Carlsson at A Teknik for their manufacturing and design work, Mr. Joakim Ingemansson and co-workers at MIDROC are highly acknowledged for their help in programming whereas Mr. Thomas Kull and co-workers at PMC are appreciated for their help regarding the hydraulic equipment.

Last but not least I thank my lovely mother- and sister- in-law Almija Crnalic and Ajla Krivic, respectively, for taking care of Malte and for their huge support to me and Alma.

References

1. R.C. Reed, 'The Superalloys: Fundamentals and Applications', Cambridge University Press, 2006.
2. G. Sjöberg: 'Casting Superalloys for Structural Applications ', Proceeding of The 7th International Symposium on Superalloy 718 and Derivatives, TMS (The Minerals, Metals and Materials Society), Ed. by E. A. Ott, J. R. Groh, A. Banik, I. Dempster, T. P. Gabb, R. Helmink, X. Liu, A. Mitchell, G. P. Sjöberg, and A. Wusatowska-Sarnek, Pittsburg, USA, October, 2010, pp. 117-130.
3. G. Sjöberg, J. Andersson, and A. Sjunnesson: Proceedings of International Society for Airbreathing Engines (ISABE), Montreal, Canada, September, 2009, n.1286.
4. 'ASM Specialty Handbook[®] - Heat Resistant Materials', ed by J. R. Davis, ASM International[®] Materials Park, Ohio, USA, April, 1999, ISBN 0-87170-596-6.
5. W.D. Cao: 'Nickel-Base Alloy', U.S. Patent 6,730,264 B2, May 04, 2004.
6. R. L. Kennedy: 'Allvac 718Plus, Superalloy for The Next Forty Years', Superalloys 718, 625, 706 and Various Derivatives, TMS, Warrendale, PA, 2005, pp. 1-14.
7. L. M. Pike: 'Development of a fabricable Gamma – Prime (γ') Strengthened Superalloy', Superalloys 2008 eds. R.C. Reed, K.A. Green, P. Caron, T. P. Gabb, M. G. Fahrman, E. S. Huron, S. A. Woodard, The Minerals, Metals & Materials Society, 2008, pp. 191-200.
8. J. Andersson: 'Allvac 718Plus – Microstructure after Heat Treatment and Welding', Report number E 3305, Department of Materials Engineering, University of Dalarna, Borlänge Sweden, 2005.
9. R.L. Kennedy, W.D. Cao, T.D. Bayha, and R. Jeniski: 'Developments in Wrought Nb Containing Superalloys (718 + 100 F°)', published in the Proceedings of the International Symposium on Niobium for High Temperature Applications, Araxá, MG, Brazil, December 01-03, 2003.
10. W.D. Cao, and R.L. Kennedy: 'Role of Chemistry in 718 Type Alloys - Allvac[®] 718 Plus[™] Development', Superalloy 2004, Seven Springs Conference, Seven Springs, PA, TMS, 2004.
11. W.D. Cao, and R.L. Kennedy: 'New Developments in Wrought 718-Type Superalloys', Acta Metallurgica Sinica, **17**, 2004.

12. H. J. White: 'The effect of Aging Heat Treatments on the Mechanical Properties of Nickel Based Superalloy Weld Metal', Proceedings of the Welding and Fabrication Technology for New Power Plants: 1st International Electrical Power Research Institute Conference, 2008.
13. M.D. Rowe: 'Ranking the Resistance of Wrought Superalloys to Strain-Age Cracking', Welding Journal, **85**, 2006, pp. 27-34.
14. G. Chirieleison, L. Snyder, and H. J. White: 'The Effect of Ageing Heat Treatments on the Mechanical Properties of Nickel Based Superalloy Welds', Proceeding of the 47th Annual Conference of Metallurgists of CIM, Aerospace Materials & Manufacturing - Advances in Processing & Repair of Aerospace Materials In Honor of Dr. Mahesh Chaturvedi, Winnipeg, Manitoba, Canada, August 24-27, 2008, pp. 223-234.
15. J. N. DuPont, J. C. Lippold, and S. D. Kiser: 'Welding Metallurgy and Weldability of Nickel-Base Alloys', John Wiley & Sons Inc., USA, 2009.
16. T. Finton, and J. C. Lippold: 'Comparison of Weld Hot Cracking Tests – Summary of an IIW Round Robin Study', EWI Report No. MR0205, 2002.
17. C. T. Sims, N. S. Stoloff, and W. C. Hagel: 'Superalloys II', John Wiley & Sons, 1987.
18. M. J. Donachie, and S.J. Donachie, Superalloys: 'Superalloys - A Technical Guide', ASM International, 2002.
19. A. Mitchell: 'Manufacture of Specialty Alloys', Lecture Presentation Slides, The Royal Institute of Technology, Stockholm, Sweden, June, 2008.
20. G. E. Dieter: 'Mechanical Metallurgy, SI Metric Edition', McGraw-Hill, 1988.
21. Special Metals Corporation: 'INCONEL[®] Alloy 718 Product Brochure', Publication Number SMC-045, September, 2007.
22. ATI ALLVAC: 'ATI 718 Plus[®] Alloy Product Brochure', Publication Number NI-417 VERSION 1, 2010.
23. Special Metals Corporation: 'Waspaloy Alloy Product Brochure', Publication Number SMC-011, September, 2004.
24. Haynes International Inc.: 'HAYNES[®] 282[®] Alloy Product Brochure', Publication Number H-3173, 2008.

25. D. F. Paulonis, J. M. Oblak, and D. S. Duvall: 'Precipitation in Nickel base Alloy 718', Transactions of American Society of Metals, **62**, 1969, p. 611.
26. R. Cozar, and A. Pineau: 'Morphology of gamma prime and gamma double prime precipitates and thermal stability of Inconel 718 type alloy', Metallurgical Transactions, **4**, 1973, p. 47.
27. G. A. Zickler, R. Radis, R. Schnitzer, E. Kozeschnik, M. Stockinger, and H. Leitner: 'The Precipitation Behavior of Superalloy ATI Allvac 718Plus', Advanced Engineering Materials, **12**, 2010, pp. 176-183.
28. L. A. Jackman, H. B. Canada, and F. E. Sczerzenie: 'Quantitative carbon partitioning diagrams for waspaloy and their application to chemistry modifications and processing', Superalloys 1980, Ed. J. K. Tien, S. J. Wlodek, H. Morrow, M. Gell, and G. E. Maurer, G.E.), 1980, p.365.
29. J. F. Radavich: 'The physical metallurgy of cast and wrought Alloy 718', Superalloy 718 - Metallurgy and Applications, Ed. E. A. Loria, 1989, p. 229.
30. K. Vishwakarma: 'Microstructural Analysis of Weld Cracking in 718 Plus Superalloy', PhD thesis, University of Manitoba, Winnipeg, Canada, 2007.
31. J. Andersson, S. Hatami, and G. Sjöberg: 'Notch Sensitivity and Intergranular Crack Growth in the Allvac 718Plus Superalloy', Proc. of 18th International Symposium on Air Breathing Engines, Beijing, China, September, 2007, paper 1293.
32. S. Azadian, L. Wei, and R Warren: 'Delta phase precipitation in Inconel 718', Materials Characterisation, **53**, 2004: p. 7.
33. T. J. Kelly: 'Investigation of elemental effects on the weldability of cast nickel-based superalloys', Advances in Welding Science and Technology, Ed. by S. A. David, Metals Park, OH, ASM International, 1986, pp. 623-627.
34. T. J. Kelly: 'Elemental Effects on the Cast 718 Weldability', Welding Journal, **68**, 1989, pp. 44-51.
35. J. J. Schirra, R. H. Caless, and R. W. Hatala: 'The effect of laves phase on mechanical properties of wrought and cast + HIP Inconel 718', Superalloys 718, 625, 706 and Various Derivatives, TMS, Warrendale, PA, 1991, p.375.
36. D. Srinivasan: 'Effect of long-time exposure on the evolution of minor phases in alloy 718', Material Science and Engineering A, **364** (1-2), 2004, pp. 27-34.

37. W. D. Callister Jr.: 'Material Science and Engineering – An Introduction', 7th ed., John Wiley & Sons, 2007.
38. J. F. Lancaster: 'Metallurgy of Welding', 6th ed., Abington Publishing, 1999.
39. S. Kou: 'Welding Metallurgy', 2nd ed., John Wiley and Sons, 2003.
40. N. L. Richards, M. C. Chaturvedi, Y. G. Liu, and K. Mount: 'Optimization of electron beam welding parameters for Incoloy 903', International journal of materials and product technology, **11** (3-4), 1996, p. 284.
41. N. L. Richards, and M. C. Chaturvedi: 'The influence of electron-beam welding parameters on Heat-Affected-Zone Microfissuring in Incoloy 903', Metallurgical and Materials Transactions A, **25**, 1994, p. 1733.
42. W. S. Pellini: 'Strain theory of hot tearing', Foundry, **80**, 1952, p. 125.
43. W. I. Pumphrey, and P. H. Jennings: 'A Consideration of the Nature of Brittleness at Temperatures above the Solidus in Castings and Welds in Aluminum Alloys', J. Inst. Metals, **75**, 1948, p. 235.
44. J. C. Borland: 'Generalized theory of super-solidus cracking in welds (and castings)', British Welding Journal, **7**, 1960, pp. 508-512.
45. D. G. Eskin, and L. Katgerman: 'A quest for a new hot tearing criterion', Metallurgical transactions A, **38**, 2007, pp. 1511-1519.
46. C. E. Cross: 'On the Origin of Weld Solidification cracking', Hot Cracking Phenomena in Welds, ed. T. Böllinghaus, and H. Herold, Springer-Verlag Berlin Heidelberg, 2005, pp. 3-18.
47. C. E. Cross, and N. Coniglio: 'Weld Solidification Cracking: Critical Conditions for Crack Initiation and Growth', Hot Cracking Phenomena in Welds II, ed. T. Böllinghaus, H. Herold, C. E. Cross, and J. C. Lippold, Springer-Verlag Berlin Heidelberg, 2008, pp. 39-58.
48. K. A. Yushchenko, and V. S. Savchenko: 'Classification and Mechanisms of Cracking in Welding High-Alloy Steels and Nickel Alloys in Brittle Temperature Ranges', Hot Cracking Phenomena in Welds II, ed. T. Böllinghaus, H. Herold, C. E. Cross, and J. C. Lippold, Springer-Verlag Berlin Heidelberg, 2008, pp. 95-114.
49. H. Fredriksson, and U. Åkerlind: 'Materials Processing During Casting', John Wiley & Sons, 2006.

50. K. Easterling: 'Introduction to the physical metallurgy of welding'. Butterworth-Heinemann, 1992.
51. M. C. Maguire, and J. R. Michael: 'Weldability of alloys 718, 625, and variants', Superalloys 718, 625, 706 and Various Derivatives, TMS, Warrendale, PA, 1994, pp. 881-892.
52. M. J. Cieslak, T. J. Headley, and A. D. Romig: 'The welding metallurgy of Hastelloy alloys C-4, C-22 and C-276', Metallurgical Transactions A, **17**, 1986, pp. 2035-2047.
53. C. V. Robino, J. R. Michael, and M. J. Cieslak: 'Solidification and welding metallurgy of thermo-span alloy', Science and Technology of Welding and Joining, **2**, 1997, pp. 220-230.
54. M. J. Cieslak: 'The welding and solidification metallurgy of Alloy 625', Welding Journal, **70**, 1991, pp. 49-56.
55. J. N. DuPont: 'Solidification of an Alloy 625 Weld Overlay', Metallurgical Transactions A, **27**, 1996, pp. 3612-3620.
56. G. A. Knorovsky, M. J. Cieslak, T. J. Headley, A. D. Romig, and W. F. Hammett: 'INCONEL 718: A solidification diagram', Metallurgical Transactions A, **20**, 1989, pp. 2149-2158.
57. M. J. Cieslak, G. A. Knorovsky, T. J. Headley, and A. D. Romig: 'The use of New PHACOMP in understanding the solidification microstructure of nickel base alloy weld metal', Metallurgical Transactions A, **17**, 1986, pp. 2107-2116.
58. M. J. Cieslak, T. J. Headley, G. A. Knorovsky, A. D. Romig Jr., and T. Kollie: 'A comparison of the solidification behavior on incoloy 909 and inconel 718', Metallurgical Transactions A, **21**, 1990, pp. 479-488.
59. M. J. Cieslak, T. J. Headley, T. Kollie, and A. D. Romig: 'A melting and solidification study of Alloy 625', Metallurgical Transactions A, **19**, 1988, pp. 2319-2331.
60. J. N. DuPont, J. R. Michael, and B. D. Newbury: 'Welding metallurgy of alloy HR-160' Welding Journal, **78**, 1999, pp. 408-414.
61. S. W. Banovic, and J. N. DuPont: 'Dilution and microsegregation in dissimilar metal welds between super austenitic stainless steels and Ni base alloys', Science and Technology of Welding and Joining, **6**, pp. 374-383.

62. J. N. DuPont, C. V. Robino, R. E. Mizia, and D. B. Williams: 'Physical and welding metallurgy of Gd-enriched austenitic alloys for spent nuclear fuel applications-part II: nickel base alloys', *Welding Journal*, **83**, pp. 289-300.
63. J. N. DuPont, C. V. Robino, and A. R. Marder: 'Solidification and weldability of Nb-bearing superalloys', *Welding Journal*, **77**, 1988, pp. 417-431.
64. J. N. DuPont, C. V. Robino, and A. R. Marde: 'Modeling solute redistribution and microstructural development in fusion welds of Nb bearing superalloys', *Acta Metallurgica*, **46**, 1988, pp. 4781-4160.
65. C. Huang, and S. Kou: 'Liquation cracking in partial-penetration aluminum welds-effect of penetration oscillation and backfilling', *Welding Journal*, **82**, 2003, pp. 184-194.
66. O.A. Idowu, O.A. Ojo, and M.C. Chaturvedi: 'Effect of heat input on heat affected zone cracking in laser welded ATI Allvac 718Plus superalloy', *Materials Science and Engineering A*, **454-455**, 2007, pp. 389-397.
67. J. C. Lippold, J. Sowards, J. Alexandrov, B. T. Murray, and A. J. Ramirez: 'Weld Solidification Cracking in Solid Solution Strengthened Ni-Base Filler Metals', *Hot Cracking Phenomena in Welds II*, ed. T. Böllinghaus, H. Herold, C. E. Cross, and J. C. Lippold, Springer-Verlag Berlin Heidelberg, 2008, pp.147 -170.
68. R. G. Thompson, J. J. Cassimus, D. E. Mayo, and J.R. Dobbs: 'The relationship between grain size and microfissuring in Alloy 718', *Welding Journal*, **64**, 1985, pp. 91-96.
69. L. Viskari, and K. Stiller: 'Atom probe tomography of Ni-base superalloys Allvac 718Plus and Alloy 718', *Ultramicroscopy*, 2011, Article in Press (doi:10.1016/j.ultramic.2011.01.015).
70. J. J. Pepe, and W. F. Savage: 'Effects of constitutional liquation in 18-Ni maraging steel weldments', *Welding Journal*, **46**, 1967, pp. 411-422.
71. W. A. Owczarski, D. S. Duvall, and C. P. Sullivan: 'Further heat-affected zone studies in heat resistant nickel alloys', *Welding Journal*, **46**, 1967, pp. 423-432.
72. B. Radhakrishnan, and R. G. Thompson: 'A phase diagram approach to study liquation cracking in alloy 718', *Metallurgical Transactions A*, **22**, 1991, pp. 887-902.

73. H. R. Zhang, and O. A. Ojo: 'Non-equilibrium liquid phase dissolution of δ phase precipitates in a nickel-based superalloy', *Philosophical Magazine Letters*, **89**, 2009, pp. 787-794.
74. W. A. Owczarski, D. S. Duvall, and C. P. Sullivan: 'A model for heat affected zone cracking in nickel base superalloys', *Welding Journal*, **45**, 1966, pp. 145-155.
75. R. Vincent: 'Precipitation around welds in the nickel-base superalloy Inconel 718', *Acta Metallurgica*, **33**, 1985, pp. 1205-1216.
76. M. C. Chaturvedi, N. L. Richards, and A. Saranchuk, in 'Superalloys 718, 625, 706 and Various Derivatives', Ed. E. Loria, TMS, 1997, pp. 743-751.
77. W. Chen, M. C. Chaturvedi, and N. L. Richards: 'Effect of B Segregation at GBs on HAZ Cracking in Wrought Inconel 718', *Metall. Mater. Trans. A.*, **32**, 2001, pp. 931-939.
78. K. Vishwakarma, N. L. Richards, and M. C. Chaturvedi: 'Microstructural analysis of fusion and heat affected zones in electron beam welded ALLVAC[®] 718PLUS[™] superalloy', *Material Science and Engineering A*, **480**, 2008, pp. 517-528.
79. K. Vishwakarma, and M. C. Chaturvedi: 'A Study of Haz Microfissuring in a Newly Developed Allvac[®] 718Plus[™] Superalloy', *Superalloys 2008*, Ed. R. C. Reed et al, pp. 241-250.
80. G. R Thompson, J.R. Dobbs, and D. E. Mayo: 'The effect of heat treatment on microfissuring in Alloy 718', *Welding Journal*, **65**, 1986, pp. 299-304.
81. W. F. Savage, E. F. Nippes, and G. M. Goodwin: 'Effect of minor elements on hot-cracking tendencies of Inconel 600', *Welding Journal*, **56**, 1977, pp. 245-253.
82. R. G. Thompson, B. Radhakrishnan, and D. E. Mayo: 'Grain Boundary Chemistry Contributions to Intergranular Hot Cracking', *Journal de Physique, Colloque C5*, **10**, pp. 471-479.
83. G. R. Pease: 'The practical welding metallurgy of nickel and high nickel alloys', *Welding Journal*, **36**, 1957, pp. 330-334.
84. H. Guo, M. C. Chaturvedi, and N. L. Richards: 'Effect of sulphur on hot ductility and heat affected zone microfissuring in Inconel 718 welds', *Science and Technology of Welding and Joining*, **5**, 2000, pp. 378-384.

85. R. G. Thompson: 'Microfissuring of alloy 718 in the weld heat affected zone', *Journal of Metals*, **40**, 1988, pp. 44-48.
86. D. S. Duvall, and W. A. Owczarski: 'Further HAZ studies in heat-resistant nickel alloys', *Welding Journal*, **46**, 1967, pp. 423-432.
87. E. G. Thompson: 'Hot cracking studies of alloy 718 weld heat-affected zones', *Welding Journal*, **48**, 1969, pp. 70-79.
88. W. A. Baeslack III, and D. E. Nelson: 'Morphology of Weld Heat-Affected Zone Liquefaction in cast alloy 718', *Metallography*, **19**, 1986, pp. 371-379.
89. C. Boucher, D. Varela, M. Dadian, and H. Granjon: 'Hot Cracking and Recent Progress in the Weldability of the Nickel Alloys Inconel 718 and Waspaloy', *Revue de Metallurgie*, **73**, 1976, pp. 817-831.
90. M. Qian: 'An Investigation of The Repair Weldability of Waspaloy and Alloy 718', PhD thesis, The Ohio State University, Columbus, USA, 2002.
91. R. Vincent: 'Precipitation Around Welds in the Nickel-Base Superalloy Inconel 718', *Acta Metallurgica*, **33**, 1985, pp. 1205-1216.
92. N. L. Richards, and M. C. Chaturvedi: 'Effect of minor elements on weldability of nickel base superalloys', *International Materials Review*, **45**, 2000, pp. 109-129.
93. M. Qian, and J. C. Lippold: 'The effect of multiple PWHTs cycles on the weldability of Waspaloy', *Welding Journal*, **81**, 2002, pp. 233-238.
94. Z. Li, S. L. Gobbi, and J. H. Loreau: 'Laser Welding of Waspaloy sheets for aero-engines', *Journal of Materials Processing*, **65**, 1997, pp. 183-190.
95. W. A. Owczarski: 'Process and metallurgical factors in joining superalloys and other high service temperature materials', *Physical Metallurgy of metal joining*, Metallurgical Society of AIME, 1980, pp.166-189.
96. A. J. Ramirez, and J. C. Lippold: 'High temperature cracking in nickel-base weld metal, Part 2-Insight into the mechanism', *Materials Science and Engineering A*, **380**, 2004, pp. 245-258.
97. M. S. Prager, and C. S. Shira: 'Welding of Precipitation-hardening Nickel- base superalloys', *Welding Research Council Bulletin* **128**, 1968.
98. D. McKeown: 'Re-heat Cracking in High Nickel Alloy Heat-Affected Zone', *Welding Journal*, **50**, 1971, pp. 201-206.

99. J. C. Lippold: 'Recent Developments in Weldability Testing', Hot Cracking Phenomena in Welds, ed. T. Böllinghaus, and H. Herold, Springer-Verlag Berlin Heidelberg, 2005, pp. 271-290.
100. W. Lin, J. C. Lippold, and W. A. Baeslack: 'Analysis of weldability testing techniques for HAZ liquation cracking', Advancements in synthesis and processes, Toronto, Canada, 1992, p. M464.
101. J. C. M. Farrar: 'Hot Cracking Tests – The Route to International Standardization', Hot Cracking Phenomena in Welds, ed. T. Böllinghaus, and H. Herold, Springer-Verlag Berlin Heidelberg, 2005, pp. 291-304.
102. L. Karlsson, E. L. Bergquist, S. Rigdal, and N. Thalberg: 'Evaluating Hot Cracking Susceptibility of Ni-Base SAW Consumables for Welding of 9% Ni Steel', Hot Cracking Phenomena in Welds II, ed. T. Böllinghaus, H. Herold, C. E. Cross, and J. C. Lippold, Springer-Verlag Berlin Heidelberg, 2008, pp. 329-347.
103. J. Jacobsson: 'Solidification Cracking Tests – Provningsmetoder för Stelningssprickor', Master Thesis, Chalmers University of Technology, Göteborg, Sweden, 2007.
104. E. F. Nippes, and W. F. Savage: 'Development of Specimen Simulating Weld Heat-Affected Zones', Welding Journal, **28**, 1949, pp. 534-546.
105. C. D. Lundin: 'Historical Development of the High Speed Time-Temperature Controller Designed for Welding Research - The Gleeble', 7th Annual ISPS Conference, Tsukuba, Japan, **January**, 1997, pp.283-289.
106. C. D. Lundin, C. Y. P. Qiao, and C.H. Lee: 'Standardization of gleeble hot ductility testing: Part1: Historical review', Weldability of Materials, Detroit, Michigan, USA, 1990, pp. 1-8.
107. C. D. Lundin, C. Y. P. Qiao, T. P. S. Gill, and G. M. Goodwin: 'Hot ductility and hot cracking behavior of modified 316 stainless steels designed for high-temperature service', welding journal, **72**, 1993, pp 189-200.
108. W. Yeniscavich: 'Correlation of Hot Ductility curves with cracking during welding', Proceeding of Symposium on Methods of High Alloy Weldability Evaluation, WRC, New York, N.Y., 1969.
109. Swedish standards institute: 'Destructive Tests on Welds in Metallic Materials – Hot Cracking Tests for Weldments – Arc Welding Processes – Part 3: Externally Loaded Tests', (ISO/TR 17641-3:2005), pp. 5-9.

110. C. D. Lundin, C. Y. P. Qiao, and C. H. Lee: 'Standardization of Gleeble hot ductility testing: Part II: Experimental Evaluation', Weldability of Materials, Detroit, Michigan, USA, 1990: pp. 9-22.
111. W. F. Savage, and C. D Lundin: 'The varestraint test', Welding Journal, **44**, 1965, pp. 433-442.
112. C. D. Lundin, A. C. Lingenfelter, G. E. Grotke, G. G. Lessmann, and S. J. Mathews: 'The Varestraint Test', Welding Research Council Bulletin **280**, August, 1982, pp 1-19.
113. Aerospace Material Specification: 'AMS 5706K', SAE International, **August**, 2002.
114. Aerospace Material Specification: 'AMS 5544H', SAE International, **April**, 2006.